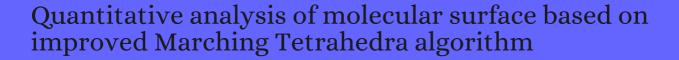
CITATION REPORT List of articles citing



DOI: 10.1016/j.jmgm.2012.07.004 Journal of Molecular Graphics and Modelling, 2012, 38, 314-23

Source: https://exaly.com/paper-pdf/53870586/citation-report.pdf

Version: 2024-04-10

This report has been generated based on the citations recorded by exaly.com for the above article. For the latest version of this publication list, visit the link given above.

The third column is the impact factor (IF) of the journal, and the fourth column is the number of citations of the article.

#	Paper	IF	Citations
1070	A B3LYP and MP2 theoretical investigation on the cooperativity effect between the XH?HM (X=F, Cl, Br; M=Li, Na, K) dihydrogen-bonding and HM?Interactions involving C6H6. 2013 , 1020, 81-90		7
1069	Revealing the nature of intermolecular interaction and configurational preference of the nonpolar molecular dimers (H贝(N即and (H风N) 2013 , 19, 5387-95		78
1068	A theoretical investigation into the cooperativity effect between the HID and HIP? interactions and electrostatic potential upon 1:2 (F?:N-(Hydroxymethyl)acetamide) ternary-system formation. 2013 , 19, 5171-85		7
1067	The geometry and electronic structure of Aristolochic acid: possible implications for a frozen resonance. 2013 , 26, 473-483		119
1066	Understanding the effects of the number of pyrazines and their positions on charge-transport properties in silylethynylated N-heteropentacenes. 2014 , 20, 2502		4
1065	Host-guest interactions in ExBox4+. 2014 , 15, 4108-16		15
1064	Theoretical insight into the coordination of cyclic D-glucose to [Al(OH)(aq)](2+) and [Al(OH)2(aq)](1+) ions. 2014 , 118, 13890-902		18
1063	Significant evidence of CIIIO and CIIIC long-range contacts in several heterodimeric complexes of CO with CH3-X, should one refer to them as carbon and dicarbon bonds!. 2014 , 16, 17238-52		51
1062	Metal- and Ligand-Supported Reduction of the {Fe2S2} Cluster as a Path to Formation of Molecular Group 13 Element Complexes {Fe2S2M} (M = Al, Ga). 2014 , 33, 2713-2720		7
1061	1,3-Cationic alkylidene migration of nonclassical carbocation: a density functional theory study on gold(I)-catalyzed cycloisomerization of 1,5-enynes containing cyclopropene moiety. 2014 , 136, 1505-13	3	36
1060	Computational Study on Cycloisomerization/Oxidative Dimerization of Aryl Propargyl Ethers Catalyzed by Gold Nanoclusters: Mechanism and Selectivity. 2014 , 33, 6633-6642		13
1059	Gas storage potential of ExBox⊞ and its Li-decorated derivative. 2014 , 16, 21964-79		10
1058	A novel photo-responsive azobenzene-containing nanoring host for fullerene-guest facile encapsulation and release. 2014 , 16, 27053-64		21
1057	Halogen bonding interaction of chloromethane with several nitrogen donating molecules: addressing the nature of the chlorine surface Ehole. 2014 , 16, 19573-89		34
1056	Trinuclear alkyl hydrido rare-earth complexes supported by amidopyridinato ligands: synthesis, structures, C-Si bond activation and catalytic activity in ethylene polymerization. 2014 , 43, 14450-60		11
1055	Exploring the nature of interactions among thiophene, thiophene sulfone, dibenzothiophene, dibenzothiophene sulfone and a pyridinium-based ionic liquid. 2014 , 16, 10531-8		13
1054	Molecular dynamics investigation of the effect of solvent adsorption on crystal habits of hexogen. 2014 , 92, 849-854		18

(2015-2014)

1053	Theoretical study of solvent effects on RDX crystal quality and sensitivity using an implicit solvation model. 2014 , 20, 2326	4
1052	Theoretical insights into the hostguest interactions between [6]cycloparaphenyleneacetylene and its anthracene-containing derivative and fullerene C70. 2014 , 27, 772-782	32
1051	Wavefunction and reactivity study of benzo[a]pyrene diol epoxide and its enantiomeric forms. 2014 , 25, 1521-1533	177
1050	Theoretical study of the structures, stabilities, and electronic properties of neutral and anionic Ca2Si \blacksquare (n = 1 \blacksquare , \blacksquare 0, +1) clusters. 2014 , 68, 1	2
1049	The comparison of cation⊞nion interactions of phosphonium- and ammonium-based ionic liquids ☐ A theoretical investigation. 2014 , 597, 114-120	10
1048	Synthesis, X-ray investigation and DFT calculations of solvated barium Ediketonate complexes with 18-dibenzocrown-6: [Ba(pta)2(18DBC6)](C6H5CH3)2 and [Ba(pta)2(18DBC6)](CH2Cl2) (pta = 1,1,1-trifluoro-5,5-dimethylhexanedionato-2,4; 18DBC6 = 18-dibenzocrown-6). 2014 , 79, 229-238	2
1047	Is Aerogen-Interaction Capable of Initiating the Noncovalent Chemistry of Group 18?. 2015 , 10, 2615-8	19
1046	Hexahalogenated and their mixed benzene derivatives as prototypes for the understanding of halogen halogen intramolecular interactions: New insights from combined DFT, QTAIM-, and RDG-based NCI analyses. 2015 , 36, 2328-43	17
1045	Multiple Cycloaddition Reactions of Ketones with a Diketiminate Al Compound. 2015, 21, 19041-7	5
1044	Adsorption, Thermodynamic and Quantum Chemical Studies of 1-hexyl-3-methylimidazolium Based Ionic Liquids as Corrosion Inhibitors for Mild Steel in HCl. 2015 , 8, 3607-3632	72
1043	From Stiba- and Bismaheteroboroxines to N,C,N-Chelated Diorganoantimony(III) and Bismuth(III) Cations-An Unexpected Case of Aryl Group Migration. 2015 , 54, 6010-9	20
1042	Sequential metalation of benzene: electronic, bonding, magnetotropic and spectroscopic properties of coinage metalated benzenes studied by DFT. 2015 , 21, 153	4
1041	A theoretical investigation on the metalinetal interaction in a series of pyrazolate bridged platinum(II) complexes. 2015 , 205, 222-227	11
1040	The effects of extended conjugation length of purely organic phosphors on their phosphorescence emission properties. 2015 , 17, 19096-103	16
1039	Fluorines in tetrafluoromethane as halogen bond donors: Revisiting address the nature of the fluorine's Bole. 2015 , 115, 453-470	36
1038	Nature of Noncovalent Interactions in the [n]Cycloparaphenylene?C70(n= 10, 11, and 12) HostQuest Complexes: A Theoretical Insight into the Shortest C70Qarbon Nanotube Peapod. 2015, 119, 5168-5179	32
1037	Synthesis, X-ray diffraction, and density functional studies of tin(IV) compounds containing a pincer-type SNS ligand. 2015 , 26, 189-198	2
1036	New insights into the nitroaromatics-detection mechanism of the luminescent metal-organic framework sensor. 2015 , 44, 2897-906	47

1035	Theoretical prediction of the host-guest interactions between novel photoresponsive nanorings and C60: a strategy for facile encapsulation and release of fullerene. 2015 , 36, 518-28	13
1034	Lewis-acid induced disaggregation of dimeric arylantimony oxides. 2015 , 51, 5932-5	22
1033	Effective utilization of noncovalent interaction descriptor in BX3Ilewis base complexes: A determination of adduct/van der Waals complexes and reassessment of the BX3 acid strength order. 2015 , 636, 117-120	6
1032	A theoretical investigation of substituent effects on the stability and reactivity of N-heterocyclic olefin carboxylates. 2015 , 13, 8533-44	24
1031	Computational study on aromaticity and resonance structures of substituted BODIPY derivatives. 2015 , 1068, 117-122	10
1030	Theoretical exploration of the nanoscale host-guest interactions between $[n]$ cycloparaphenylenes $(n = 10, 8 \text{ and } 9)$ and fullerene Clifrom single- to three-potential well. 2015 , 17, 18802-12	36
1029	Some Quinoxalin-6-yl Derivatives as Corrosion Inhibitors for Mild Steel in Hydrochloric Acid: Experimental and Theoretical Studies. 2015 , 119, 16004-16019	301
1028	The hydrogen storage capacity of coinage metalated benzenes studied by DFT. 2015 , 68, 2653-2665	1
1027	Towards understanding the decomposition/isomerism channels of stratospheric bromine species: ab initio and quantum topology study. 2015 , 16, 6783-800	6
1026	Atmospheric nucleation precursors catalyzed isomerization of CH2SH to CH3S: mechanisms and topological analysis. 2015 , 26, 261-268	4
1025	Benzimidazole-Containing Porous Organic Polymers as Highly Active Heterogeneous Solid-Base Catalysts. 2015 , 7, 1559-1565	26
1024	Geometries, stabilities and electronic properties of small-sized Pd2-doped Sin (n = 1111) clusters. 2015 , 113, 3567-3577	4
1023	Designation and Exploration of Halide-Anion Recognition Based on Cooperative Noncovalent Interactions Including Hydrogen Bonds and Anion-II 2015 , 119, 5842-52	21
1022	Theoretical Study on the Rational Design of Cyano-Substituted P3HT Materials for OSCs: Substitution Effect on the Improvement of Photovoltaic Performance. 2015 , 119, 8501-8511	33
1021	A New Graphdiyne Nanosheet/Pt Nanoparticle-Based Counter Electrode Material with Enhanced Catalytic Activity for Dye-Sensitized Solar Cells. 2015 , 5, 1500296	149
1020	Intramolecularly Group 15 Stabilized Aryltellurenyl Halides and Triflates. 2015 , 34, 5341-5360	21
1019	Cell membrane causes the lipid bilayers to behave as variable capacitors: A resonance with self-induction of helical proteins. 2015 , 207, 114-27	7
1018	Application-oriented computational studies on a series of D-EA structured porphyrin sensitizers with different electron-donor groups. 2015 , 17, 30624-31	4

(2016-2015)

1017	Understanding the Boron-Nitrogen Interaction and Its Possible Implications in Drug Design. 2015 , 119, 14393-401	5
1016	Alkali and alkaline-earth atom-decorated B38 fullerenes and their potential for hydrogen storage. 2015 , 40, 13022-13028	29
1015	Microwave spectroscopic and theoretical investigations of the strongly hydrogen bonded hexafluoroisopropanol water complex. 2015 , 17, 24774-82	16
1014	Unusual bonding modes of perfluorobenzene in its polymeric (dimeric, trimeric and tetrameric) forms: entirely negative fluorine interacting cooperatively with entirely negative fluorine. 2015 , 17, 31624-45	28
1013	Intriguing properties of unusual silicon nanocrystals. 2015 , 5, 78192-78208	23
1012	Theoretical studies of traditional and halogen-shared halogen bonds: the doped all-metal aromatic clusters MAl3 [[M = Si, Ge, Sn, Pb) as halogen bond acceptors. 2015 , 134, 1	1
1011	Comparative study on the methods for predicting the reactive site of nucleophilic reaction. 2015 , 58, 1845-1852	56
1010	Roles of hydrogen bonds and latacking in the optical detection of nitro-explosives with a luminescent metal of granic framework as the sensor. 2015 , 5, 3045-3053	55
1009	Experimental and theoretical studies of CH?M interactions in palladium and platinum complexes derived from 1,2-bis-(2-hydroxymethylphenylthio)ethane. 2015 , 87, 181-193	9
1008	Deprotonation-triggered Stokes shift fluorescence of an unexpected basic-stable metal-organic framework. 2015 , 54, 65-8	18
1007	The importance of molecular conformation to the properties: a DFT study of the polynitro heterocyclic compounds based on dodecahydrodiimidazo [4,5-b:4?,5?-e]pyrazine structure. 2015 , 26, 667-674	3
1006	Theoretical investigation on activation of CH and CC bonds of 2-butyne by gas-phase Nb atom. 2016 , 1085, 23-30	6
1005	Germylenes and stannylenes stabilized within N2PE rings (E = Ge or Sn): combined experimental and theoretical study. 2016 , 45, 10343-54	5
1004	Molecular partitioning based on the kinetic energy density. 2016 , 652, 40-45	2
1003	Functionalization of fullerene via the Bingel reaction with ⊞-chlorocarbanions: an ONIOM approach. 2016 , 22, 113	4
1002	Experimental and theoretical studies on some selected ionic liquids with different cations/anions as corrosion inhibitors for mild steel in acidic medium. 2016 , 64, 252-268	93
1001	Theoretical insight into the sensitive mechanism of multilayer-shaped cocrystal explosives: compression and slide. 2016 , 22, 108	1
1000	Cellobiose as a model system to reveal cellulose dissolution mechanism in acetate-based ionic liquids: Density functional theory study substantiated by NMR spectra. 2016 , 149, 348-56	26

999	Adsorption Behavior of Glucosamine-Based, Pyrimidine-Fused Heterocycles as Green Corrosion Inhibitors for Mild Steel: Experimental and Theoretical Studies. 2016 , 120, 11598-11611	313
998	Reactivity of electrophilic chlorine atoms due to Eholes: a mechanistic assessment of the chemical reduction of a trichloromethyl group by sulfur nucleophiles. 2016 , 18, 27300-27307	7
997	Theoretical insight into the temperature-dependent acetonitrile (ACN) solvent effect on the diacetone diperoxide (DADP)/1,3,5-tribromo-2,4,6-trinitrobenzene (TBTNB) cocrystallization. 2016 , 121, 232-239	8
996	Acyclic ⊞-Phosphinoamido-Germylene: Synthesis and Characterization. 2016 , 35, 3635-3640	8
995	Theoretical investigation on activation of ethene by the HNbNIanion in the gas phase. 2016 , 1096, 74-79	1
994	A mechanistic study on guanidine-catalyzed chemical fixation of CO2 with 2-aminobenzonitrile to quinazoline-2,4(1H,3H)-dione. 2016 , 3, 823-835	25
993	Direct siliconflitrogen bonded host materials with enhanced Itonjugation for blue phosphorescent organic light-emitting diodes. 2016 , 4, 10047-10052	16
992	Fluorinated antimony(v) derivatives: strong Lewis acidic properties and application to the complexation of formaldehyde in aqueous solutions. 2016 , 7, 6768-6778	47
991	Adsorption and corrosion inhibition properties of N-{n-[1-R-5-(quinoxalin-6-yl)-4,5-dihydropyrazol-3-yl]phenyl}methanesulfonamides on mild steel in 1 M HCl: experimental and theoretical studies. 2016 , 6, 86782-86797	98
990	Anion-Controlled Positional Switching of a Phenyl Group about the Dinuclear Core of a AuSb Complex. 2016 , 55, 9162-72	31
989	Probing the structures, stabilities, and electronic properties of neutral and charged carbon-doped lithium CLi \ln (n = 200, \pm 0, \pm 1) clusters from unbiased CALYPSO method. 2016 , 51, 9440-9454	5
988	Comparing Nucleophilicity of Heavier Heteroleptic Amidinato-Amido Tetrelylenes: An Experimental and Theoretical Study. 2016 , 1, 1991-1995	5
987	Theoretical investigation on exciton-dissociation and charge-recombination processes of PC61BM-PTDPPSe interface. 2016 , 22, 241	1
986	Theoretical Prediction on Photovoltaic Properties of 4Cl-BPPQ/PC61BM System via Density Functional Theory Calculations. 2016 , 34, 1143-1150	4
985	Computational modelling of panchromatic porphyrins with strong NIR absorptions for solar energy capture. 2016 , 665, 40-46	3
984	2,4-Diamino-5-(phenylthio)-5H-chromeno [2,3-b] pyridine-3-carbonitriles as green and effective corrosion inhibitors: gravimetric, electrochemical, surface morphology and theoretical studies. 2016 , 6, 53933-53948	116
983	Computational Studies on the Mo-Doped Gold Nanoclusters Au n Mo(n = 1🗓0): Structures, Stabilities and Magnetic Properties. 2016 , 27, 993-1004	3
982	Theoretical characterization on photovoltaic properties of PC61BM-PTDPPTFT4 system with a molecular model. 2016 , 1089, 6-12	

(2017-2016)

981	Electrochemical, Theoretical, and Surface Morphological Studies of Corrosion Inhibition Effect of Green Naphthyridine Derivatives on Mild Steel in Hydrochloric Acid. 2016 , 120, 3408-3419	214
980	Can an entirely negative fluorine in a molecule, viz. perfluorobenzene, interact attractively with the entirely negative site(s) on another molecule(s)? Like liking like!. 2016 , 6, 19098-19110	35
979	Comparison of the directionality of the halogen, hydrogen, and lithium bonds between HOOOH and XF (XI=ICl, Br, H, Li). 2016 , 22, 52	4
978	Fluorine substitution effects of halide anion receptors based on the combination of a distinct hydrogen bond and anion[honcovalent interactions: a theoretical investigation. 2016 , 6, 14666-14677	9
977	5-Arylpyrimido-[4,5-b]quinoline-diones as new and sustainable corrosion inhibitors for mild steel in 1 M HCl: a combined experimental and theoretical approach. 2016 , 6, 15639-15654	108
976	Theoretical study of the catalytic oxidation mechanism of 5-hydroxymethylfurfural to 2,5-diformylfuran by PMo-containing Keggin heteropolyacid. 2016 , 6, 3776-3787	27
975	Theoretical Study of Geometries, Stabilities, and Electronic Properties of Cationic (FeS)n+ (n = 18) Clusters. 2016 , 71, 45-51	3
974	Synthesis, crystal structure, spectroscopic properties and DFT calculations of a new Schiff base-type Zinc(II) complex. 2016 , 42, 3473-3488	32
973	Quinoxaline derivatives as corrosion inhibitors for mild steel in hydrochloric acid medium: Electrochemical and quantum chemical studies. 2016 , 76, 109-126	90
972	Theoretical investigation on photovoltaic properties of PC61BM-PDPP5T system as a promising polymer-based solar cell. 2017 , 30, e3592	
971	Effect of additional donor group on the charge transfer/recombination dynamics of a photoactive organic dye: A quantum mechanical investigation. 2017 , 1103, 38-47	18
970	Prediction of excited-state properties of oligoacene crystals using polarizable continuum model-tuned range-separated hybrid functional approach. 2017 , 38, 569-575	25
969	Anion Recognition Based on a Combination of Double-Dentate Hydrogen Bond and Double-Side Anion-[Noncovalent Interactions. 2017 , 121, 892-900	17
968	What is the effect of carbon nanotube shape on desalination process? A simulation approach. 2017 , 407, 103-115	21
967	Systematic analysis of structural and topological properties: new insights into $PuO2(H2O)n2+ (n = 1B)$ complexes in the gas phase. 2017 , 7, 4291-4296	7
966	A Theoretical Perspective on the Photovoltaic Performance of S,N-Heteroacenes: An Even t dd Effect on the Charge Separation Dynamics. 2017 , 121, 2574-2587	38
965	Study of the mechanism of the catalytic decomposition of hydrogen iodide (HI) over carbon materials for hydrogen production. 2017 , 42, 4977-4986	7
964	Liquid-phase exfoliation (LPE) of graphite towards graphene: An ab initio study. 2017 , 230, 461-472	29

963	The Analysis of Electronic Structures, NBO, EDA, and QTAIM of trans-(H3P)2(12-BH4)W(?C-para-C6H4X)(CO) Complexes. 2017 , 64, 369-378	5
962	Theoretical investigation effects of anchor groups on photovoltaic properties for the C217-based dye sensitizer. 2017 , 1105, 89-96	9
961	Topological analysis of steric and relaxation deformation densities. 2017 , 115, 743-756	6
960	Experimental and theoretical investigation of the inhibitory effect of new pyridazine derivatives for the corrosion of mild steel in 1 M HCl. 2017 , 1136, 127-139	63
959	Van Der Waals heterogeneous layer-layer carbon nanostructures involving IIIH-C-C-HIIIIIH-C-C-H stacking based on graphene and graphane sheets. 2017 , 38, 730-739	12
958	A general strategy to enhance the alkaline stability of anion exchange membranes. 2017 , 5, 6318-6327	39
957	Counterion-induced crystallization of intermetalloid Matryoshka clusters [Sb@Pd@Sb]. 2017, 46, 3453-3456	16
956	Evolution of the interaction between C20 cage and Cr(CO)5: A solvent effect, QTAIM and EDA investigation. 2017 , 16, 1750007	3
955	Mechanisms and Origins of Chemo- and Regioselectivities of Ru(II)-Catalyzed Decarboxylative C-H Alkenylation of Aryl Carboxylic Acids with Alkynes: A Computational Study. 2017 , 139, 7224-7243	112
954	Reactions between hydroxyl-substituted alkylperoxy radicals and Criegee intermediates: correlations of the electronic characteristics of methyl substituents and the reactivity. 2017 , 19, 15073-15083	13
953	The Analysis of Os?C Bond and Electric Field Influence on the Properties in the Osmium Carbyne Complex OsCl3 (?CCH2CMe3)(PH3)2: A Theoretical Insight. 2017 , 64, 651-657	16
952	Structural, spectral, electrochemical and DFT studies of two mononuclear manganese(II) and zinc(II) complexes. 2017 , 122, 228-240	88
951	Theoretical Investigation into Suitable Pore Sizes of Membranes for Vanadium Redox Flow Batteries. 2017 , 4, 2184-2189	18
950	Time dependent density functional theory characterization of organic dyes for dye-sensitized solar cells. 2017 , 43, 1523-1531	13
949	Pnicogen bond interaction between PF2Y (Y = \square ?N, \square ?C) with NH3, CH3OH, H2O, and HF molecules. 2017 , 28, 1843-1851	3
948	Experimental, quantum chemical and molecular dynamic simulations studies on the corrosion inhibition of mild steel by some carbazole derivatives. 2017 , 7, 2436	51
947	Hydrogen-bridge Si(EH)3CeH and inserted H3SiCeH molecules: Matrix infrared spectra and DFT calculations for reaction products of silane with Ce atoms. 2017 , 1146, 692-702	5
946	Corannulene f ullerene C70 noncovalent interactions and their effect on the behavior of charge transport and optical property. 2017 , 7, 27960-27968	7

945	Reaction mechanism of hydrogen cyanide catalyzed by gas-phase titanium. 2017 , 117, e25412	2
944	Synthesis and evaluation of aromaticity and tautomerization of pyrazolopyridazin(on)es. 2017 , 129, 741-752	5
943	Theoretical investigation into the influence of molar ratio on binding energy, mechanical property and detonation performance of 1,3,5,7-tetranitro-1,3,5,7-tetrazacyclo octane (HMX)/1-methyl-4,5-dinitroimidazole (MDNI) cocrystal explosive. 2017 , 1109, 27-35	8
942	A density functional theory study on the interactions between dibenzothiophene and tetrafluoroborate-based ionic liquids. 2017 , 23, 145	9
941	Experimental and theoretical study on the molecular structure, covalent and non-covalent interactions of 2,4-dinitrodiphenylamine: X-ray diffraction and QTAIM approach. 2017 , 1141, 53-63	11
940	DFT study on the dissolution mechanisms of ⊞-cyclodextrin and chitobiose in ionic liquid. 2017 , 169, 227-235	18
939	Theoretical Study of Substituent Effects on Geometric and Spectroscopic Parameters (IR, 13C, 29Si NMR) and Energy Decomposition Analysis of the Bonding in Molybdenum Silylidyne Complexes CpMo(CO)2(?Si-para-C6H4X). 2017 , 64, 522-530	14
938	Noncovalent interactions from electron density topology and solvent effects on spectral properties of Schiff bases. 2017 , 175, 134-144	18
937	Activation of acetonitrile by gas-phase uranium: bond structure analysis and spinflip reaction mechanism. 2017 , 136, 1	
936	Mechanism and Origins of Ligand-Controlled Stereoselectivity of Ni-Catalyzed Suzuki-Miyaura Coupling with Benzylic Esters: AlComputational Study. 2017 , 139, 12994-13005	78
935	Facile activation of alkynes with a boraguanidinato-stabilized germylene: a combined experimental and theoretical study. 2017 , 46, 12339-12353	8
934	Ph(R)IF?HF (R = Me, Et, i Pr, t Bu) interaction: A strong hydrogen bond between hypervalent iodine compounds and HF. 2017 , 1118, 45-52	1
933	Responsive mechanism of three novel hypochlorous acid fluorescent probes and solvent effect on their sensing performance *. 2017 , 26, 083102	1
932	Phosphorene quantum dot-fullerene nanocomposites for solar energy conversion: An unexplored inorganic-organic nanohybrid with novel photovoltaic properties. 2017 , 685, 16-22	19
931	Theoretical insight into the solvent effect of HO and formamide on the cooperativity effect in HMX complex. 2017 , 23, 237	3
930	Biopolymer from Tragacanth Gum as a Green Corrosion Inhibitor for Carbon Steel in 1 M HCl Solution. 2017 , 2, 3997-4008	40
929	A Computational Understanding of Solvent Effect on the Structure, Electronic, Thermochemical, and Spectroscopic Properties of Ni(12-C6H4)(H2PCH2CH2PH2) Complex. 2017 , 64, 925-933	3
928	Unravelling hydrogen bonding interactions of tryptamine-water dimer from neutral to cation. 2017 , 19, 25260-25269	6

927	Molecular interactions between 1-butyl-3-methylimidazolium tetrafluoroborate and model naphthenic acids: A DFT study. 2017 , 243, 462-471	19
926	Substituent Effect on the Electronic Properties and Nature of the W?C Bond in trans-Cl(OC)(H3P)3W(?C-para-C6H4X) (X = H, F, SiH3, CN, NO2, SiMe3, CMe3, NH2, NMe2) Complexes: A Computational Quantum Chemistry Study. 2017 , 64, 1340-1346	16
925	Supramolecular architecture of 5-bromo-7-methoxy-1-methyl-1 H -benzoimidazole.3H 2 O: Synthesis, spectroscopic investigations, DFT computation, MD simulations and docking studies. 2017 , 1149, 602-612	7
924	S-Enantiomer of the Antitubercular Compound S006-830 Complements Activity of Frontline TB Drugs and Targets Biogenesis of Cell Envelope. 2017 , 2, 8453-8465	9
923	Growth morphology of CL-20/HMX cocrystal explosive: insights from solvent behavior under different temperatures. 2017 , 23, 360	18
922	A combined experimental and theoretical approach for structural, spectroscopic, NLO, NBO, thermal and photophysical studies of new fluorescent 5-amino-1-(7-chloroquinolin-4-yl)-1H-1,2,3-triazole-4-carbonitrile using density functional theory.	9
921	Enhanced aerobic degradation of 4-chlorophenol with iron-nickel nanoparticles. 2017, 393, 316-324	50
920	Modeling Photovoltaic Performances of BTBPD-PC61BM System via Density Functional Theory Calculations. 2017 , 30, 268-276	1
919	Nucleophilicities of Lewis Bases B and Electrophilicities of Lewis Acids A Determined from the Dissociation Energies of Complexes B?A Involving Hydrogen Bonds, Tetrel Bonds, Pnictogen Bonds, Chalcogen Bonds and Halogen Bonds. 2017 , 22,	21
918	Implications of monomer deformation for tetrel and pnicogen bonds. 2018 , 20, 8832-8841	55
917	Solid-State Photodimerization of Azaanthracene Derivative Based on a [4+4] Cycloaddition. 2018 , 7, 906-909	4
916	Theoretical study of an anti-Markovnikov addition reaction catalyzed by Etyclodextrin. 2018, 24, 77	2
915	Extractive Distillation Approach to the Removal of Dimethyl Disulfide from Methyl Tert-Butyl Ether: Combined Computational Solvent Screening and Experimental Process Investigation. 2018 , 57, 3348-3358	11
914	Theoretical investigation on the electronic structures and spectroscopic properties as well as the features as dyes in dye-sensitized solar cells of quinonoid containing Re(I) complexes. 2018 , 862, 40-52	11
913	Predicting ion mobility collision cross sections directly from standard quantum chemistry software. 2018 , 53, 432-434	2
912	Spectroscopic and Electronic Analysis of Chelation Reactions of Galangin and Related Flavonoids with Nickel(II). 2018 , 63, 1488-1497	5
911	Remote modulation of singlet E riplet gaps in carbenes. 2018 , 694, 48-52	2
910	A combined electrochemical and theoretical study of pyridine-based Schiff bases as novel corrosion inhibitors for mild steel in hydrochloric acid medium. 2018 , 130, 1	29

909	Interactions of Biodegradable Ionic Liquids with a Model Naphthenic Acid. 2018, 8, 176	9
908	Adsorption characteristics of green 5-arylaminomethylene pyrimidine-2,4,6-triones on mild steel surface in acidic medium: Experimental and computational approach. 2018 , 8, 657-670	26
907	Three-dimensional nanopores on monolayer graphene for hydrogen storage. 2018 , 209, 134-145	5
906	Crystal lattice free volume in a study of initiation reactivity of nitramines: Friction sensitivity. 2018 , 14, 132-136	5
905	Cost-effective synthesis of carbazole/triphenylsilyl host materials with multiple Iltonjugation for blue phosphorescent organic light-emitting diodes. 2018 , 151, 187-193	6
904	Aerogen bonds formed between AeOF (Ae = Kr, Xe) and diazines: comparisons between Ehole and Ehole complexes. 2018 , 20, 4676-4687	24
903	Gravimetric, Electrochemical, Surface Morphology, DFT, and Monte Carlo Simulation Studies on Three N-Substituted 2-Aminopyridine Derivatives as Corrosion Inhibitors of Mild Steel in Acidic Medium. 2018 , 122, 11870-11882	56
902	Improvement of photovoltaic performances by optimizing £conjugated bridge for the C217-based dyes: A theoretical perspective. 2018 , 360, 137-144	2
901	Electron transfer and charge transport of photoelectric material in external electric field. 2018 , 199, 278-284	6
900	Combined spectroscopic, DFT, TD-DFT and MD study of newly synthesized thiourea derivative. 2018 , 1155, 184-195	16
900 899		16 2
	2018 , 1155, 184-195	
899	2018, 1155, 184-195 Asymmetrical semisphere nanopores on monolayer graphene for gas permeation. 2018, 53, 1962-1977 Understanding of the conformational flexibility and electrostatic properties of coumarin	2
899 898	2018, 1155, 184-195 Asymmetrical semisphere nanopores on monolayer graphene for gas permeation. 2018, 53, 1962-1977 Understanding of the conformational flexibility and electrostatic properties of coumarin derivatives in the active site of S. cerevisiae ∃-glucosidase. 2018, 27, 607-617 The role of the Eholes in stability of non-bonded chalcogenidebenzene interactions: the ground	2 O
899 898 897	Asymmetrical semisphere nanopores on monolayer graphene for gas permeation. 2018, 53, 1962-1977 Understanding of the conformational flexibility and electrostatic properties of coumarin derivatives in the active site of S. cerevisiae ℍ-glucosidase. 2018, 27, 607-617 The role of the Eholes in stability of non-bonded chalcogenidebenzene interactions: the ground and excited states. 2017, 20, 299-306 Experimental and spin-orbit coupled TDDFT predictions of photophysical properties of three-coordinate mononuclear and four-coordinate binuclear copper(I) complexes with	2 O 8
899 898 897 896	Asymmetrical semisphere nanopores on monolayer graphene for gas permeation. 2018, 53, 1962-1977 Understanding of the conformational flexibility and electrostatic properties of coumarin derivatives in the active site of S. cerevisiae \(\text{\tex{\tex	2 0 8
899 898 897 896	Asymmetrical semisphere nanopores on monolayer graphene for gas permeation. 2018, 53, 1962-1977 Understanding of the conformational flexibility and electrostatic properties of coumarin derivatives in the active site of S. cerevisiae \(\text{H-glucosidase}. \) 2018, 27, 607-617 The role of the Eholes in stability of non-bonded chalcogenidebenzene interactions: the ground and excited states. 2017, 20, 299-306 Experimental and spin-orbit coupled TDDFT predictions of photophysical properties of three-coordinate mononuclear and four-coordinate binuclear copper(I) complexes with thioamidines and bulky triarylphosphanes. 2018, 471, 680-690 Does gold cluster promote or scavenge radicals? A controversy at DFT. 2018, 31, e3776 Modification on C217 by auxiliary acceptor toward efficient sensitiser for dye-sensitised solar cells:	2 0 8 5

891	A comparative view on the potential acting on an electron in a molecule and the electrostatic potential through the typical halogen bonds. 2018 , 39, 573-580	21
890	Probing the geometries and electronic properties of charged Zr2Si n q (n = 1 1 2, q = 1 1) clusters. 2018 , 29, 139-146	2
889	Thermochemical and conformational study of optical active phenylbenzazole derivatives. 2018 , 116, 7-20	5
888	Influences of the substituents on the Cr=C bond in [(OC)5Cr=C(OEt)-para-C6H4X] complexes: quantum Theory of Atoms in Molecules, Energy Decomposition Analysis, and Interacting Quantum Atoms. 2018 , 149, 2167-2174	6
887	Theoretical Study of the Arene Ligand Effect on the Structure and Properties of Cr(CO)3(Arene) Complexes (Arene = Benzene, Biphenyl, Triphenly, Tetraphenyl). 2018 , 59, 1784-1790	3
886	Theoretical Study of the Solvent Effect on the Electronic and Vibrational Properties of [CpFe(CO)2(NCS)] and [CpFe(CO)2(SCN)] Linkage Isomers. 2018 , 59, 1058-1066	1
885	Theoretical Study of NO Linkage Isomers in a Rhenacarborane Nitrosyl Complex. 2018 , 92, 2518-2523	
884	Liquid Diquid Extraction of Benzene Using Low Transition Temperature Mixtures: COSMO-SAC Predictions and Experiments. 2018 ,	2
883	What kind of neutral halogen bonds can be modulated by solvent effects?. 2018 , 20, 26126-26139	14
882	Coordination diversity in tin compounds with bis(benzoxazole)phenol as a polydentate ligand: Synthesis and crystal structure studies. 2018 , 71, 3790-3805	1
881	Study of ($\{\text{CD}\}_{5}^{+}$) lons and Deuterated Variants(($\{\text{C}\}_{\{\{\text{Ext}\{H\}\}\}_{x}\}_{x}\}_{x}\}_{x}$) (5 - x))}^{ + })): An Artefactual Rotation. 2018 , 92, 2215-2226	
880	Triel-Bonded Complexes between TrR (Tr=B, Al, Ga; R=H, F, Cl, Br, CH) and Pyrazine. 2018 , 19, 3122-3133	18
879	Spectroscopic profiling (FT-IR, FT-Raman, NMR and UV-Vis), autoxidation mechanism (H-BDE) and molecular docking investigation of 3-(4-chlorophenyl)-N,N-dimethyl-3-pyridin-2-ylpropan-1-amine by DFT/TD-DFT and molecular dynamics: A potential SSRI drug. 2018 , 77, 131-145	19
878	Electrochemical oxidation of pyrrole, pyrazole and tetrazole using a TiO2 nanotubes based SnO2-Sb/3D highly ordered macro-porous PbO2 electrode. 2018 , 826, 181-190	23
877	Mechanistic insights into the catalytic role of various acid sites on ZSM-5 zeolite in the carbonylation of methanol and dimethyl ether. 2018 , 8, 3193-3204	21
876	X-ray structures, spectroscopic, electrochemical, thermal, antibacterial, and DFT studies of two nickel(II) and cobalt(III) complexes constructed from a new quinazoline-type ligand. 2018 , 32, e4426	18
875	Theoretical investigation on the gas phase decomposition of ethyl acetate by Ni+. 2018, 29, 1449-1456	2
874	Enantioseparation of fluorinated 3-arylthio-4,4'-bipyridines: Insights into chalcogen and Ehole bonds in high-performance liquid chromatography. 2018 , 1567, 119-129	16

873	Probing the geometries and electronic properties of iridium-doped silicon (mathrm{Ir}_{2}mathrm{Si}_{n} (n=1-18)) clusters. 2018 , 133, 1	2
872	Influence of Solvent and Electric Field on the Structure and IR, 31P NMR Spectroscopic Properties of a Titanocene B enzyne Complex. 2018 , 85, 526-534	13
871	Supramolecular structures of rhenium(I) complexes mediated by ligand planarity via the interplay of substituents. 2018 , 74, 997-1006	10
870	First-principles and Molecular Dynamics simulation studies of functionalization of Au golden fullerene with amino acids. 2018 , 8, 11400	14
869	Halogen Bonding in Ring-Substituted Group 10 POCOP Iodido Complexes with Iodine and Its Possible Role in Oxidative Addition. 2018 , 2018, 3913-3921	3
868	Theoretical insight into the structure and bonding characteristics of Bisphenol-A. QTAIM and NBO analyses. 2018 , 17, 1850034	
867	Density Functional Theory Investigations of D-A-D' Structural Molecules as Donor Materials in Organic Solar Cell. 2018 , 6, 200	9
866	Substructure-activity relationship studies on antibody recognition for phenylurea compounds using competitive immunoassay and computational chemistry. 2018 , 8, 3131	13
865	Regium bonds between M clusters (M = Cu, Ag, Au and n = 2-6) and nucleophiles NH and HCN. 2018 , 20, 22498-22509	36
864	Theoretical modeling of argentophilic interactions in [Ag(CN)2]B trimer found in a copper(II) complex of cis-1,2-diaminocyclohexane (Dach), [Cu(Dach)2-Ag(CN)2-Cu(Dach)2][Ag(CN)2]3. 2018 , 709, 11-15	4
863	New Insights into Adsorption Behaviour of NH3 Molecules on Small (SiO2)n (n=211) Clusters Through Systematic Analysis of Structural and Topological Properties. 2018 , 71, 482	1
862	Vibrational and electronic absorption spectroscopic profiling, natural hybrid orbital, charge transfer, electron localization function and molecular docking analysis on 3-amino-3-(2-nitrophenyl) propionic acid. 2018 , 1171, 733-746	17
861	Origin of Different Photovoltaic Activities in Regioisomeric Small Organic Molecule Solar Cells: The Intrinsic Role of Charge Transfer Processes. 2018 , 122, 14296-14303	16
860	Synthesis, structural characterization, spectroscopic, and DFT studies of two penta-coordinated zinc(II) complexes containing quinazoline and 1, 10-phenanthroline as mixed ligands. 2018 , 203, 234-246	31
859	Noncovalent interactions between O6-corona[6]arene nanorings and fullerenes C60 and C70: atypical ring ball-shaped host-guest systems. 2019 , 32, e3892	3
858	Why do AIT and GIC self-sort? Hilkel aromaticity as a driving force for electronic complementarity in base pairing. 2019 , 17, 1881-1885	5
857	Shape and non-bonding interactions in the formic acid-difluoromethane complex by rotational spectroscopy. 2019 , 206, 185-189	6
856	Computational study on C1- versus C3-regioselectivity in Pd(II)-catalyzed olefination/dearomatization of 2-naphthyl ureas. 2019 , 477, 110540	

855	Multimolecular Complexes of CL-20 with Nitropyrazole Derivatives: Geometric, Electronic Structure, and Stability. 2019 , 4, 13408-13417	6
854	High-efficiency pure blue thermally activated delayed fluorescence emitters with a preferentially horizontal emitting dipole orientation via a spiro-linked double DA molecular architecture. 2019 , 7, 10851-10859	33
853	Tuning of the conformation of asymmetric nonfullerene acceptors for efficient organic solar cells. 2019 , 7, 22279-22286	47
852	Electron transfer and intersystem crossing triggered fluorescence quenching detection of mercury ions. 2019 , 21, 16676-16685	6
851	The role of hydrogen bonding in literactions in Ni(II) complex derived from triethanolamine: synthesis, crystal structure, antimicrobial, and DFT studies. 2019 , 45, 5649-5664	6
850	Investigation on 4-amino-5-substituent-1,2,4-triazole-3-thione Schiff bases an antifungal drug by characterization (spectroscopic, XRD), biological activities, molecular docking studies and electrostatic potential (ESP). 2019 , 1197, 171-182	14
849	Synthesis, characterization, spectral property, Hirshfeld surface analysis and TD/DFT calculations of 2, 6-disubstituted benzobisoxazoles. 2019 , 1197, 508-518	13
848	Extraction and stripping of platinum (IV) from acidic chloride media using guanidinium ionic liquid. 2019 , 293, 111040	15
847	Noncovalent Close Contacts in Fluorinated Thiophenel Phenylenel Thiophene Conjugated Units: Understanding the Nature and Dominance of Oll wersus Slift and Oll Interactions with Respect to the Control of Polymer Conformation. 2019 , 31, 7070-7079	12
846	Antimicrobial activities of self-assembled copper(II), nickel(II), and cobalt(III) complexes combined with crystallographic, spectroscopic, DFT calculations and Hirshfeld surfaces analyses. 2019 , 43, 12417-12430	25
845	A 3D Analogue of Phenyllithium: Solution-Phase, Solid-State, and Computational Study of the Lithiacarborane [Li-CB H]. 2019 , 58, 19007-19013	8
844	pH-Responsive Switching Properties of a Water-Soluble Metallamacrocyclic Phenylalaninehydroximate La(III)ជ្រu(II) Complex: Insight into Tuning Protonation Ligand States. 2019 , 2019, 4328-4335	3
843	Deep eutectic solvents based highly efficient extractive desulfurization of fuels Œco-friendly approach. 2019 , 296, 111916	62
842	Structural and Computational Insights into Cocrystal Interactions: A Case on Cocrystals of Antipyrine and Aminophenazone. 2019 , 19, 6175-6183	17
841	Aromaticity and Induced Current Study of C8H ($n+2$)8 ($n=B$, A , B , A , B): In the Viewpoint of Huckel B Rule. 2019 , 60, 1361-1374	2
840	Development of an off-on selective fluorescent sensor for the detection of Fe3+ ions based on Schiff base and its Hirshfeld surface and DFT studies. 2019 , 296, 111814	15
839	Solvent Influence on Structure and Electronic Properties of Si2Me4: A Computational Investigation Using PCM-SCRF Method. 2019 , 93, 2244-2249	4
838	Theoretical Studies of IR and NMR Spectral Changes Induced by Sigma-Hole Hydrogen, Halogen, Chalcogen, Pnicogen, and Tetrel Bonds in a Model Protein Environment. 2019 , 24,	23

837	A 3D Analogue of Phenyllithium: Solution-Phase, Solid-State, and Computational Study of the Lithiacarborane [Lithiacarborane	1
836	Electronic effect of Biketonato ligands on the redox potential of fac and mer tris(Biketonato) iron(III) complexes: A density functional theory study and molecular electrostatic potential analysis. 2019 , 119, e26036	6
835	Characterization of a MnII complex of Alizarin suggests attributes explaining a superior anticancer activity: A comparison with anthracycline drugs. 2019 , 173, 114104	3
834	Double-bond elucidation for arsagermene with a tricoordinate germanium center: a theoretical survey. 2019 , 43, 15681-15690	Ο
833	Chalcogen bonding of two ligands to hypervalent YF (Y = S, Se, Te, Po). 2019 , 21, 20829-20839	15
832	Impact of cyanide co-ligand to convert crystal structure of pyrazole-based copper coordination compounds from a dinuclear to a polymeric structure and DFT calculations of [Cu2(tpmp)X2] (X = Cl and I). 2019 , 497, 119082	7
831	A density functional theory study on complexation processes and intermolecular interactions of triptycene-derived oxacalixarenes. 2019 , 138, 1	15
830	Theoretical study of the ligand effect on NHCdobalt-catalyzed hydrogenation of ketones. 2019 , 9, 5315-5321	3
829	The synergistic effect and microscopic mechanism of co-adsorption of three emerging contaminants and copper ion on gemini surfactant modified montmorillonite. 2019 , 184, 109610	11
828	Understanding the axial chirality control of quinidine-derived ammonium cation-directed O-alkylation: a computational study. 2019 , 17, 1916-1923	6
827	Novel aryloxyphenoxypropionate derivates containing benzofuran moiety: Design, synthesis, herbicidal activity, docking study and theoretical calculation. 2019 , 154, 78-87	11
826	Spontaneous single-crystal to single-crystal transition with self-healing cracks involving solvent exchange. 2019 , 21, 1102-1106	6
825	Introducing Asymmetry Induced by Benzene Substitution in a Rigid Fused Spacer of DA-Type Solar Cells: A Computational Investigation. 2019 , 123, 4007-4021	33
824	Interaction between the plant alkaloid berberine and fullerene C70: Experimental and quantum-chemical study. 2019 , 278, 452-459	10
823	Experimental and theoretical investigations of cyclometalated ruthenium(ii) complex containing CCC-pincer and anti-inflammatory drugs as ligands: synthesis, characterization, inhibition of cyclooxygenase and in vitro cytotoxicity activities in various cancer cell lines. 2019 , 48, 728-740	18
822	A Comparison of NH 2+5 and CH +5 Ions and Deuterated Variants of NHxD 2+(5lk): Real or Artefactual Rotation?. 2019 , 60, 713-726	
821	Gain-of-Function SHP2 E76Q Mutant Rescuing Autoinhibition Mechanism Associated with Juvenile Myelomonocytic Leukemia. 2019 , 59, 3229-3239	25
820	Theoretical explanation for the pharmaceutical incompatibility through the cooperativity effect of the drug-drug intermolecular interactions in the phenobarbital paracetamol BO complex. 2019 , 25, 181	2

819	The first water-soluble polynuclear metallamacrocyclic Sr(ii)-Cu(ii) complex based on simple glycinehydroximate ligands. 2019 , 48, 10479-10487	4
818	Anion-binding properties of Electron deficient cavity in tetraoxacalix[2]arene[2]triazine by a computational study. 2019 , 288, 111007	2
817	Nano Molecular Motor of Azo Antibiotics on Edge-Carboxylated Graphene: A UV and Visible-Switchable Sensors. 2019 , 93, 324-332	
816	Computational evaluation of the reactivity and pharmaceutical potential of an organic amine: A DFT, molecular dynamics simulations and molecular docking approach. 2019 , 222, 117188	31
815	A Theoretical Approach towards Identification of External Electric Field Effect on (Б-С5Н5)Ме2Та(Г2-С6Н4). 2019 , 93, 482-487	5
814	Interactions of (MY)6 (M = Zn, Cd; Y = O, S, Se) quantum dots with N-bases. 2019 , 30, 1003-1014	O
813	Experimental, DFT dimeric modeling and AIM study of H-bond-mediated composite vibrational structure of Chelidonic acid. 2019 , 5, e01586	9
812	Charge transport and transfer phenomena involving conjugated acenes and heteroacenes. 2019 , 42, 1	1
811	Amoxicillin on polyglutamic acid composite three-dimensional graphene modified electrode: Reaction mechanism of amoxicillin insights by computational simulations. 2019 , 1073, 22-29	16
810	Influence of monomer deformation on the competition between two types of Eholes in tetrel bonds. 2019 , 21, 10336-10346	17
809	Theoretical Study of the Interaction between Graphyne and cis-PtCl2(NH3)2 Complex. 2019, 64, 369-376	О
808	Removing phenol contaminants from wastewater using graphene nanobuds: DFT and reactive MD simulation investigations. 2019 , 286, 110872	6
807	Spectroscopic, electrochemical and electrocolorimetric properties of novel 2-(2?-pyridyl)-1H-benzimidazole appended bay-substituted perylene diimide triads. 2019 , 379, 54-62	6
806	Density Functional Theory Descriptors for Ionic Liquids and the Introduction of a Coulomb Correction. 2019 , 123, 4188-4200	10
805	Theoretical design of a fluorescence sensor with configuration-transformed metal ion recognition of aza-18-crown-6. 2019 , 31, 402-411	
804	Mechanism and Origins of Regioselectivity of Copper-Catalyzed Borocyanation of 2-Aryl-Substituted 1,3-Dienes: A Computational Study. 2019 , 84, 5514-5523	30
803	Insight into spin-orbital interaction using MCSCF method: A special analysis of the lelectronic state in C and the linear polyacetylenic C and C. 2019 , 40, 1338-1343	2
802	Experimental and theoretical investigations of Cs adsorption on crown ethers modified magnetic adsorbent. 2019 , 371, 712-720	29

801	An ideal platform of light-emitting materials from phenothiazine: facile preparation, tunable red/NIR fluorescence, bent geometry-promoted AIE behaviour and selective lipid-droplet (LD) tracking ability. 2019 , 7, 4185-4190	16
800	Experimental and theoretical study on cetylpyridinium dipicrylamide 🖪 promising ion-exchanger for cetylpyridinium selective electrodes. 2019 , 1187, 77-85	19
799	Rydberg state mediated multiphoton ionization of (IJCH)(IJCH)Cr: DFT-supported experimental insights into the molecular and electronic structures of excited sandwich complexes. 2019 , 21, 9665-9671	
798	A rational design of manganese electrocatalysts for Lewis acid-assisted carbon dioxide reduction. 2019 , 21, 8849-8855	10
797	CH 3 NH 3 Formed by Electron Injection at Heterojunction Inducing Peculiar Properties of CH 3 NH 3 PbI 3 Material. 2019 , 36, 026701	
796	A theoretical insight into several common anion recognitions based on double-dentate hydrogen bond and anion-Loexistence. 2019 , 32, e3959	3
795	A Novel Electrochemical Sensor Based on Silsesquioxane/Nickel (II) Phthalocyanine for the Determination of Sulfanilamide in Clinical and Drug Samples. 2019 , 31, 867-875	20
794	A probe into underlying factors affecting utrafast charge transfer at Donor/IDIC interface of all-small-molecule nonfullerene organic solar cells. 2019 , 375, 1-8	8
793	State-specific electrostatic potential descriptors for estimating solvatochromic effects. 2019 , 25, 60	2
792	Organic Compounds of Actinyls: Systematic Computational Assessment of Structural and Topological Properties in [AnO(CO)] (An = U, Np, Pu, Am; n = 1-3) Complexes. 2019 , 58, 3425-3434	8
791	Influence of nanopore density on ethylene/acetylene separation by monolayer graphene. 2019 , 21, 6126-613	2 11
790	Computational insight into the contribution of para-substituents on the reduction potential, proton affinity, and electronic properties of nitrobenzene compounds. 2019 , 25, 78	10
7 ⁸ 9	Hexacoordinated Tetrel-Bonded Complexes between TF (T=Si, Ge, Sn, Pb) and NCH: Competition between Eand EHoles. 2019 , 20, 959-966	19
788	Theoretical study of the geometrical and electronic properties of Be2Mg+ n (n = $1\overline{1}$ 1) clusters. 2019 , 9, 778-785	4
787	Removal of platinum (IV) from hydrochloric acid medium with OMImT: Theoretical and experimental evidences for a neutral complexing mechanism. 2019 , 293, 111529	0
786	Fishbone-Like Polymer from Green Cationic Polymerization of Methyl Eleostearate as Biobased Nontoxic PVC Plasticizer. 2019 , 7, 18976-18984	14
785	Modulating intramolecular chalcogen bonds in aromatic (thio)(seleno)phene-based derivatives. 2019 , 21, 23645-23650	8
7 ⁸ 4	Unraveling the regioselectivity of odd electron halogen bond formation using electrophilicity index and chemical hardness parameters. 2019 , 21, 26580-26590	8

783	Non-linear optical properties of carbazole based dyes modified with diverse spacer units for dye-sensitized solar cells: A first principle study. 2019 ,	0
782	Recovery of Au(III) from Acidic Chloride Media by Homogenous Liquid[liquid Extraction with UCST-Type Ionic Liquids. 2019 , 7, 19975-19983	13
781	Synthesis and Mechanism of Adsorption Capacity of Modified Montmorillonite with Amino Acids for 4-Acetaminophenol Removal from Wastewaters. 2019 , 64, 5900-5909	1
7 ⁸ 0	Spectroscopic, antimicrobial and computational study of novel benzoxazole derivative. 2019 , 1176, 881-894	14
779	Spectroscopic and electronic structure characterization of hydrogen bonding in 2-Bromohydroquinone. 2019 , 1181, 71-82	6
778	The interaction between chitosan and tannic acid calculated based on the density functional theory. 2019 , 520, 100-107	32
777	Evaluating Computational and Structural Approaches to Predict Transformation Products of Polycyclic Aromatic Hydrocarbons. 2019 , 53, 1595-1607	6
776	Imidazolium-based ionic liquids with inorganic anions in the extraction of salidroside and tyrosol from Rhodiola: The role of cations and anions on the extraction mechanism. 2019 , 275, 136-145	18
775	Molecular docking studies, charge transfer excitation and wave function analyses (ESP, ELF, LOL) on valacyclovir: A potential antiviral drug. 2019 , 78, 9-17	75
774	Computational study of new 1,2,3-triazole derivative of lithocholic acid: Structural aspects, non-linear optical properties and molecular docking studies as potential PTP 1B enzyme inhibitor. 2019 , 78, 144-152	4
773	Computational study of structural, vibrational and electronic properties of the highly symmetric molecules M4S6 (M = P, As, Sb, Bi). 2019 , 1149, 41-48	1
772	Interactions of promazine with selected biomolecules: Photophysical and computational investigation. 2019 , 517, 161-176	2
771	Influence of substituents on the reduction potential and pKa values of Ediketones tautomers: A theoretical study. 2019 , 297, 947-960	13
770	Multiple Ether-Functionalized Phosphonium Ionic Liquids as Highly Fluid Electrolytes. 2019 , 20, 443-455	11
769	Comparison of radical scavenging behavior of chromones dihydrogenistein and demethyltexasin DFT approach. 2019 , 30, 167-173	2
768	Quinoline derivatives as possible lead compounds for anti-malarial drugs: Spectroscopic, DFT and MD study. 2020 , 13, 632-648	71
767	Theoretical prediction of structures and inclusion properties of heteroatom-bridged pillar[n]arenes. 2020 , 31, 329-337	4
766	A sensitive sensing platform for acetaminophen based on palladium and multi-walled carbon nanotube composites and electrochemical detection mechanism. 2020 , 239, 121977	18

765 properties of tris(Ediketonato)iron(III) complexes. 2020, 31, 215-232 The interaction of 5-fluorouracil with graphene in presence of external electric field: a theoretical 764 investigation. 2020, 26, 905-911 Enhanced photovoltaic performances of C219-based dye sensitisers by introducing 763 1 electron-withdrawing substituents: a density functional theory study. 2020, 118, e1636151 Exploring the detailed spectroscopic characteristics, chemical and biological activity of two 762 53 cyanopyrazine-2-carboxamide derivatives using experimental and theoretical tools. 2020, 224, 117414 Multicomponent supramolecular assemblies of 1(2H)-Phthalazinone and Tetrafluoroterephthalic acid: Understanding the role of hydrogen bonding on the structure and properties using 761 5 experimental and computational analyses. 2020, 228, 117689 Cobalt phthalocyanine is a suitable scaffold for lithium polysulfide (Li2Sn n = 2B). 2020, 739, 136942 760 9 The single/co-adsorption characteristics and microscopic adsorption mechanism of biochar-montmorillonite composite adsorbent for pharmaceutical emerging organic contaminant 40 759 atenolol and lead ions. 2020, 187, 109763 Analysis of hydrogen bonding and weak interactions in the crystal structure of (E)-N-(4-ethylphenyl)-2-(4-hydroxybenzylidene)thiosemicarbazone: experimental and theoretical 758 studies. 2020, 118, e1670878 Heteroleptic cobalt(II) complex with nitrogen-rich macrocycles [5tructure, bioactivity and DFT 8 757 modelling. 2020, 100, 106117 Behavior, mechanism and equilibrium studies of Au(iii) extraction with an ionic liquid [C-6-CBIm]Br. 756 2020, 49, 504-510 Degradation mechanism of biphenyl and 4-4'-dichlorobiphenyl cis-dihydroxylation by non-heme 2,3 5 755 dioxygenases BphA: A QM/MM approach. 2020, 247, 125844 The conformational search, the stability, fragment interaction and resistance to acidic attack of 754 epoxyl-polyurethanes in different solvent media. **2020**, 31, 861-875 Structures and energetics of clusters surrounding diatomic anions stabilized by hydrogen, halogen, 14 753 and other noncovalent bonds. 2020, 530, 110590 A DFT study on mechanisms of CO2 coupling with propargylic alcohols using alkali carbonates. 2020 2 752 , 120, e26150 Corrections of Molecular Morphology and Hydrogen Bond for Improved Crystal Density Prediction. 4 751 2019, 25, Urease inhibition studies of six Ni(II), Co(II) and Cu(II) complexes with two sexidentate NO-donor 750 bis-Schiff base ligands: An experimental and DFT computational study. 2020, 204, 110959 Rapid removal of toxic metals Cu2+ and Pb2+ by amino trimethylene phosphonic acid intercalated 749 79 layered double hydroxide: A combined experimental and DFT study. 2020, 392, 123711 Synthesis, crystal structure, TD/DFT calculations and Hirshfeld surface analysis of 748 16 1-(4-((Benzo)dioxol-5-ylmethyleneamino)phenyl)ethanone oxime. 2020, 1204, 127552

A theoretical investigation of the fragment interaction and nonlinear optical and electronic

747	Degradation mechanism for Zearalenone ring-cleavage by Zearalenone hydrolase RmZHD: A QM/MM study. 2020 , 709, 135897	12
746	Halogen bond in separation science: A critical analysis across experimental and theoretical results. 2020 , 1616, 460788	13
745	Experimental and computational analysis of 1-(4-chloro-3-nitrophenyl)-3-(3,4-dichlorophenyl)thiourea. 2020 , 1205, 127587	29
744	Co-effects of the electron transfer and intersystem crossing on the photophysics of a phenothiazine based Hg sensor. 2020 , 229, 117939	O
743	Theoretical investigation of a cation-controllable molecular shuttle of tetracationic cyclophane. 2020 , 33, e4036	
742	The interactions between polar solvents (methanol, acetonitrile, dimethylsulfoxide) and the ionic liquid 1-ethyl-3-methylimidazolium bis(fluorosulfonyl)imide. 2020 , 299, 112159	25
741	Computational insight into energetic cage derivatives based on hexahydro-1,3,5-trinitro-1,3,5-triazine. 2020 , 67, 961-968	1
74º	Comparative study of the effects of ortho-, meta- and para-carboranes (CBH) on the physicochemical properties, cytotoxicity and antiviral activity of uridine and 2'-deoxyuridine boron cluster conjugates. 2020 , 94, 103466	5
739	Water-Soluble Bismuth(III) Polynuclear Tyrosinehydroximate Metallamacrocyclic Complex: Structural Parallels to Lanthanide Metallacrowns. 2020 , 25,	2
738	Factors Impacting Eland Electrostatic Potential and Its Source Function Reconstruction: The Case of 4,4'-Bipyridine Derivatives. 2020 , 25,	6
737	Minimizing aromatics entrainment in dephenolization of coal-based liquids by deep eutectic solvents. 2020 , 8, 100070	
736	Potential of diamines for absorption of SO2: Effect of methanol group. 2020 , 319, 114163	8
735	van der Waals potential: an important complement to molecular electrostatic potential in studying intermolecular interactions. 2020 , 26, 315	38
734	The adsorption of chlorofluoromethane on pristine and Ge-doped silicon carbide nanotube: a PBC-DFT, NBO, and QTAIM study. 2020 , 46, 1405-1416	14
733	The adsorption of chlorofluoromethane on pristine, and Al- and Ga-doped boron nitride nanosheets: a DFT, NBO, and QTAIM study. 2020 , 26, 287	11
732	Theoretical Analysis of Stereoelectronic Effects in the 2,4,6-Trihalo-1,3,5-trioxane and 2,4,6-Trihalo-1,3,5-trithiane Conformers. 2020 , 94, 2064-2071	O
731	Acceptor plane expansion enhances horizontal orientation of thermally activated delayed fluorescence emitters. 2020 , 6,	47
730	Theoretical Prediction on a Novel Reduction-Responsive Nanoring Having a Disulfide Group for Facile Encapsulation and Release of Fullerenes C and C. 2020 , 5, 25400-25407	2

729	Computational investigation of flavonol-based GLP-1R agonists using DFT calculations and molecular docking. 2020 , 1190, 113005	4
728	Low-coordinate Sm(II) and Yb(II) complexes derived from sterically-hindered 1,2-bis(imino)acenaphthene (Ar-bian). 2020 , 49, 14445-14451	6
727	Dual Functionalization of Electron Transport Layer Tailoring Molecular Structure for High-Performance Perovskite Light-Emitting Diodes. 2020 , 12, 37346-37353	10
726	Molecular Structural Properties of [n]-Annulene (n = 8, 10, 12, 14) and its Boron Nitride Derivatives: Analysis of NMR, NBO, ELF and PDI. 2020 , 61, 207-224	
725	1-Hydroxymethyl-3,5-dimethylpyrazole: Coordination with Ba (II), Hg (II) and DFT studies. 2020 , 31, S134-S140	0
724	Computational Rationalization of the Interaction of Fe(CO)4 and Substituted Benzyne Ligands. 2020 , 61, 197-206	O
723	Synthesis and thermal properties of magnetite nano structures and DFT analysis of Fe3O4 cluster as its smallest representative unit*. 2020 , 1222, 128895	1
722	Lithium isotope effect in extraction of lithium chloride by 4-Aminobenzo-15-crown-5 in water-anisole ionic liquid double solvent system. 2020 , 325, 673-682	1
721	Cyclic Voltammetric and DFT Analysis of the Reduction of Manganese(III) Complexes with 2-Hydroxybenzophenones. 2020 , 32, 2913-2925	1
720	Precise parallel volumetric comparison of molecular surfaces and electrostatic isopotentials. 2020 , 15, 11	1
719	Experiment and simulation for CO2 capture using low transition temperature mixtures as solvents. 2020 , 103, 103178	4
718	Synthesis and properties of salts derived from C4N182IIC4N18H3Iand C4N18H3Ianions. 2020 , 8, 25035-25039	6
717	-(2-Aminoethyl)-2-(hexylthio) Acetamide-Functionalized Pillar[5]arene for the Selective Detection of l-Trp through Guest-Adaptive Multisupramolecular Interactions. 2020 , 124, 9811-9817	11
716	Codeposition of Levodopa and Polyethyleneimine: Reaction Mechanism and Coating Construction. 2020 ,	14
715	Quantum Chemical Study of Interaction between Titanocene Dichloride Anticancer Drug and Al12N12 Nano-Cluster. 2020 , 65, 1726-1734	4
714	Designing high-performance hypergolic propellants based on materials genome. 2020 , 6,	13
713	A thorough theoretical exploration of the effect mechanism of Fe on HCN heterogeneous formation from nitrogen-containing char. 2020 , 280, 118662	13
7 12	Theoretical Insights into the Effect of Cations, Anions, and Water on Fixation of CO Catalyzed by Different Ionic Liquids. 2020 , 13, 6391-6400	3

Substituent effects on the structure and properties of (para-C5H4X)Ir(PH3)3 complexes in the ground state (S0) and first singlet excited state (S1): DFT and TD-DFT investigations. **2020**, 174751982094286

710	Noncovalent Bonds between Tetrel Atoms. 2020 , 21, 1934-1944	15
709	Theoretical studies on oxadiazole-based layer stacking nitrogen-rich high-performance insensitive energetic materials. 2020 , 26, 298	1
708	Room-Temperature Flexible Quasi-Solid-State Rechargeable Na-O Batteries. 2020 , 6, 1955-1963	11
707	Disubstituted Ferrocenyl Iodo- and Chalcogenoalkynes as Chiral Halogen and Chalcogen Bond Donors. 2020 , 39, 3936-3950	15
706	Structural Effects of Amines in Enhancing Methanesulfonic Acid-Driven New Particle Formation. 2020 , 54, 13498-13508	14
705	High-Performance Anion Exchange Membranes with Para-Type Cations on Electron-Withdrawing C?O Links Free Backbone. 2020 , 53, 10988-10997	14
704	Graphitic-N-rich N-doped graphene as a high performance catalyst for oxygen reduction reaction in alkaline solution. 2020 , 45, 32402-32412	19
703	ESPALIE Analysis as a Theoretical Tool for Identifying the Coordination Atoms of Possible Multisite Extractants: Validation and Prediction. 2020 , 8, 14353-14364	1
702	The conformational change of Plukenetia conophora oil derivatives and their acidic resistance, intra-fragment interactions, stability in different solvent media. 2020 , 26, 312	
701	Probing on the Stable Structure of Silicon-Doped Charged Magnesium Nanomaterial Sensor: SiMgn∃1 (N = 2¶2) Clusters DFT Study. 2020 , 7,	6
700	Theoretical study of the adsorption of amantadine on pristine, Al-, Ga-, P-, and As-doped boron nitride nanosheets: a PBC-DFT, NBO, and QTAIM study. 2020 , 139, 1	9
699	Effect of Bulky Functional Groups on Donor and Acceptor Interactions and their Photoluminescence Properties. 2020 , 21, 2620-2626	1
698	How to complete the tautomerization and substrate-assisted activation prior to CI bond fission by meta-cleavage product hydrolase LigY?. 2020 , 10, 5856-5869	
697	A theoretical study of the reactivity of ethene and benzophenone with a hyper-coordinated alkene containing a so-called E=E (E = C, Si, Ge, Sn, and Pb) unit. 2020 , 49, 12842-12853	1
696	Anomalous Melting Point of Multicharge Ionic Liquids: Structural, Electrostatic, and Orbital Properties of [Ln(NO)] (Ln = Ce, Pr) Anions. 2020 , 59, 13700-13708	1
695	Bioinspired succinyl-Eyclodextrin membranes for enhanced uranium extraction and reclamation. 2020 , 7, 3124-3135	4
694	Analysis of Bonding Properties of Osmabenzyne in the Ground State (S0) and Excited Singlet (S1) State: A Quantum-Chemical Calculation. 2020 , 94, 2594-2600	

693	Exploring the Substituent Effect on the Structure and Ectronic roperties of Si2(para-C6H4X)2 Ble cules. 2020 , 94, 2760-2769	2
692	Theoretical investigation on cis-trans isomerisation of azaphosphatriptycene- based molecular gear. 2020 , 32, 569-577	1
691	Simultaneous interlayer and intralayer space control in two-dimensional metal-organic frameworks for acetylene/ethylene separation. 2020 , 11, 6259	23
690	Volatile-char interactions during biomass pyrolysis: Contribution of amino group on graphitized carbon nanotube to xylose evolution based on experimental and theoretical studies. 2020 , 282, 118921	12
689	Ether functionalisation, ion conformation and the optimisation of macroscopic properties in ionic liquids. 2020 , 22, 23038-23056	13
688	Effect of silanol on the thermal stability of poly[methyl(trifluoropropyl)siloxane]. 2020, 137, 49347	3
687	Sulfhydryl functionalized covalent organic framework as an efficient adsorbent for selective Pb (II) removal. 2020 , 600, 125004	26
686	A potential bio-antioxidant for mineral oil from cashew nutshell liquid: an experimental and theoretical approach. 2020 , 37, 369-381	5
685	Bio-Based Antimicrobial Ionic Materials Fully Composed of Natural Products for Elevated Air Purification. 2020 , 4, 2000046	2
684	Halogen Bonding in New Dichloride-Cobalt(II) Complex with Iodo Substituted Chalcone Ligands. 2020 , 10, 354	5
683	A pillar[5]arene-based fluorescent sensor for sensitive detection of L-Met through a dual-site collaborative mechanism. 2020 , 240, 118569	8
682	Rational Design, Synthesis, Characterization and Evaluation of Iodinated 4,4'-Bipyridines as New Transthyretin Fibrillogenesis Inhibitors. 2020 , 25,	8
681	Strong chemisorption of E2H2 and E2H4 (E = C, Si) on B12N12 nano-cage. 2020 , 10, 179-191	20
680	Amino and hydroxy substitution influences pyrene-DNA binding. 2020 , 725, 138542	6
679	Influence of spin state and electron configuration on the active site and mechanism for catalytic hydrogenation on metal cation catalysts supported on NU-1000: insights from experiments and microkinetic modeling. 2020 , 10, 3594-3602	8
678	Pnicogen Bonds Pairing Anionic Lewis Acid with Neutral and Anionic Bases. 2020 , 124, 4998-5006	17
677	Sorption of five organic compounds by polar and nonpolar microplastics. 2020 , 257, 127206	30
676	Density Functional Theory Studies of the Adsorption and Interactions between Selenium Species and Mercury on Activated Carbon. 2020 , 34, 9779-9786	9

675	A comparison of ether- and alkyl-imidazolium-based ionic liquids diluted with CH3CN: A combined FTIR and DFT study. 2020 , 313, 113542	7
674	The strategy for improving the stability of nitroform derivatives-high-energetic oxidant based on hexanitroethane. 2020 , 26, 181	2
673	Molecular and dissociative adsorption of tetrachlorodibenzodioxin on M-doped graphenes ($M = B$, Al, N, P): pure DFT and DFT + VdW calculations. 2020 , 26, 164	2
672	Photodegradation of seven bisphenol analogues by Bi5O7I/UiO-67 heterojunction: Relationship between the chemical structures and removal efficiency. 2020 , 277, 119222	35
671	Comparative enantioseparation of chiral 4,4'-bipyridine derivatives on coated and immobilized amylose-based chiral stationary phases. 2020 , 1625, 461303	11
670	The effect of introducing an ether group into an imidazolium-based ionic liquid in binary mixtures with DMSO. 2020 , 22, 15734-15742	19
669	An investigation of pregabalin lactamization process and effect of various pH on reaction: A computational insight. 2020 , 1210, 128048	2
668	Models for predicting impact sensitivity of energetic materials based on the trigger linkage hypothesis and Arrhenius kinetics. 2020 , 26, 65	20
667	Experimental and DFT study of the effect of mercaptosuccinic acid on cyanide-free immersion gold deposition 2020 , 10, 9768-9776	2
666	A promising insensitive energetic material based on a fluorodinitromethyl explosophore group and 1,2,3,4-tetrahydro-1,3,5-triazine: synthesis, crystal structure and performance 2020 , 10, 11816-11822	7
665	Hammett and Brown correlations in the structure and electronic properties of H2Si=SiHAr (Ar = p-C6H4X; X = NH2, OH, Me, H, F, Cl, CHO, COOH, CN, NO2) molecules. 2020 , 67, 1348-1355	1
664	Synthesis and micro-mechanistic studies of histidine modified montmorillonite for lead(II) and copper(II) adsorption from wastewater. 2020 , 157, 142-152	21
663	Theoretical design and rotational conformation analysis of molecular bevel gear with triptycene as rotator. 2020 , 139, 1	2
662	Molecular Mechanisms and Structural Basis of Retigabine Analogues in Regulating KCNQ2 Channel. 2020 , 253, 167-181	11
661	Spectroscopy driven DFT computation for a structure of the monomeric Cu2+-Curcumin complex and thermodynamics driven evaluation of its binding to DNA: Pseudo-binding of Curcumin to DNA. 2020 , 1221, 128732	3
660	Mechanistic insights of adenine promoted activity of low-molecule tyrosine phosphatase: An ONIOM study. 2020 , 754, 137719	1
659	Adsorptive removal of diclofenac sodium from aqueous solution by magnetic COF: Role of hydroxyl group on COF. 2020 , 603, 125238	13
658	Self-Assembled Biomimetic Capsules for Self-Preservation. 2020 , 16, e2000930	2

657	Theoretical Characterization of Catalytically Active Species in Reductive Hydroxymethylation of Styrene with CO over a Bisphosphine-Ligated Copper Complex. 2020 , 59, 9667-9682	6
656	Nickel-catalyzed hydroalkenylation of styrene with phenylpropanal: theoretical studies on the mechanism, regioselectivity, and role of phenylboronic acid. 2020 , 7, 2207-2215	2
655	How Many Pnicogen Bonds can be Formed to a Central Atom Simultaneously?. 2020, 124, 2046-2056	19
654	Quantum theory of atoms in molecules, electron localization function, and localized-orbital locator investigations on trans-(NHC)PtI2(para-NC5H4X) complexes. 2020 , 44, 482-486	O
653	Absorptive Desulfurization of Model Biogas Stream Using Choline Chloride-Based Deep Eutectic Solvents. 2020 , 12, 1619	15
652	A diazabenzoperylene derivative as ratiometric fluorescent probe for cysteine with super large Stokes shift. 2020 , 412, 2687-2696	4
651	Wavefunction analysis, charge transfer and molecular docking studies on famciclovir and entecavir: Potential anti-viral drugs. 2020 , 26, 100353	2
650	Gold(III) separation from acidic medium by amine-based ionic liquid. 2020 , 304, 112735	16
649	Molecular engineering of acceptors to control aggregation for optimized nonfullerene solar cells. 2020 , 8, 5458-5466	34
648	The facile synthesis of zoledronate functionalized hydroxyapatite amorphous hybrid nanobiomaterial and its excellent removal performance on Pb and Cu. 2020 , 392, 122291	27
647	Effect of N-doping on the catalytic decomposition of hydrogen iodide over activated carbon: Experimental and DFT studies. 2020 , 45, 4511-4520	7
646	Wave function and molecular reactivity study of char with different edges and the chemisorption properties of nitric oxide. 2020 , 93, 1519-1526	5
645	Modification on the Indacenodithieno[3,2-b]thiophene Core to Achieve Higher Current and Reduced Energy Loss for Nonfullerene Solar Cells. 2020 , 32, 1297-1307	29
644	Theoretical study of adsorption of ethanol and acetone molecules by perfect and defected h-BN nanosheet. 2020 , 139, 106403	
643	Synthesis, molecular docking studies, and larvicidal activity evaluation of new fluorinated neonicotinoids against Anopheles darlingilarvae. 2020 , 15, e0227811	2
642	Competition between Intra and Intermolecular Triel Bonds. Complexes between Naphthalene Derivatives and Neutral or Anionic Lewis Bases. 2020 , 25,	16
641	On the Stability of Interactions between Pairs of Anions - Complexes of MCl (M=Be, Mg, Ca, Sr, Ba) with Pyridine and CN. 2020 , 21, 870-877	18
640	Zinc(II) and Cadmium(II) complexes containing imidazole ring: Structural, spectroscopic, antibacterial, DFT calculations and Hirshfeld surface analysis. 2020 , 507, 119610	6

639	Theoretical study on the activation of C-H bond in ethane by PdX ($X = F$, Cl, Br, H, and CH) in the gas phase. 2020 , 26, 91	
638	High-performance particulate matter including nanoscale particle removal by a self-powered air filter. 2020 , 11, 1653	50
637	Anticrystal Engineering of Ketoprofen and Ester Local Anesthetics: Ionic Liquids or Deep Eutectic Mixtures?. 2020 , 12,	10
636	Anion???Anion Attraction in Complexes of MCl (M=Zn, Cd, Hg) with CN. 2020, 21, 1119-1125	22
635	Investigation of P ropolis l s a Green Inhibitor of SAE 1010 Carbon Steel Corrosion in 3.5% NaCl Environment. 2020 , 59, 9328-9339	5
634	Gene reconstruction spandex with intrinsic antimicrobial activity. 2021 , 404, 125152	4
633	Application of a 2D-QSAR with a sine normalization method for the biodegradation of fluoroquinolones to poison cyanobacteria. 2021 , 28, 11302-11316	3
632	Complex of 4-(2-aminophenyl) 1,2,3-thiadiazole with 2,3-dichloro-5,6-dicyano-1,4-benzoquinone: Experimental study and investigation at different exchange-correlation functionals. DOS, NBO, QTAIM and RDG analyses. 2021, 1223, 128855	4
631	Vibrational, spectroscopic, chemical reactivity, molecular docking and in vitro anticancer activity studies against A549 lung cancer cell lines of 5-Bromo-indole-3-carboxaldehyde. 2021 , 34, e2873	1
630	Structural effects on thermodynamic behavior and hydrogen bond interactions of waterlbnic liquid systems. 2021 , 230, 116186	8
629	Switchable and adjustable AIE activity of Pt(II) complexes achieving swift-responding and highly sensitive oxygen sensing. 2021 , 326, 128987	8
628	The adsorption of bromochlorodifluoromethane on pristine and Ge-doped silicon carbide nanotube: a PBC-DFT, NBO, and QTAIM study. 2021 , 32, 481-494	17
627	Exploration of adsorption mechanism of 2-phosphonobutane-1,2,4-tricarboxylic acid onto kaolinite and montmorillonite via batch experiment and theoretical studies. 2021 , 403, 123810	41
626	Intermolecular interaction characteristics of the all-carboatomic ring, cyclo[18]carbon: Focusing on molecular adsorption and stacking. 2021 , 171, 514-523	104
625	Two dinuclear copper (II) and nickel (II) complexes based on 4-(diethylamino)salicylaldehyde: X-ray structures, spectroscopic, electrochemical, antibacterial, Hirshfeld surfaces analyses, and time-dependent density functional theory calculations. 2021 , 35,	5
624	Efficient absorption properties of surface grafted HEDP-HAP composites for Pb and Cu: Experimental study and visualization study of interaction based on Becke surface analysis and independent gradient model. 2021 , 401, 123748	10
623	The ratiometric detection and mechanism of three typical phosphonates by quercetin-based fluorescent probe with low detection limits. 2021 , 231, 117778	2
622	Preparative separation of high-purity trans- and cis-ferulic acid from wheat bran by pH-zone-refining counter-current chromatography. 2021 , 1636, 461772	2

(2021-2021)

621	Stabilization mechanism of arsenic-sulfide slag by density functional theory calculation of arsenic-sulfide clusters. 2021 , 410, 124567	5
620	Mechanism of transition metal cluster catalysts for hydrogen evolution reaction. 2021 , 46, 3484-3492	6
619	Investigation on the preparation of 2,2-difluoroethylamine by amination of 1-halo-2,2-difluoroethane. 2021 , 242, 109690	Ο
618	Computational study on the metabolic activation mechanism of PeCDD by Cytochrome P450 1A1. 2021 , 405, 124276	2
617	Reaction activity and mechanism of R3-CH structure oxidation in coal self-heating. 2021, 290, 119797	6
616	An Ultimate Investigation on the Adsorption of Amantadine on Pristine and Decorated Fullerenes C59X (X=Si, Ge, B, Al, Ga, N, P, and As): A DFT, NBO, and QTAIM Study. 2021 , 20, 23-39	13
615	Facile modification of hydrochar derived from cotton straw with excellent sorption performance for antibiotics: Coupling DFT simulations with experiments. 2021 , 760, 144124	11
614	Heteroatom Engineering of Hyper-Cross-Linked Polymers for Iodine Capture. 2021 , 3, 209-215	5
613	Cationic covalent organic framework for efficient removal of PFOA substitutes from aqueous solution. 2021 , 412, 127509	14
612	Spectroscopic characterization, DFT studies, molecular docking and cytotoxic evaluation of 4-nitro-indole-3-carboxaldehyde: A potent lung cancer agent. 2021 , 34, e2872	5
611	Crystal structure analysis of (E)-N-(3,5-dimethylphenyl)-2-(substituted benzylidene)thiosemicarbazone: Experimental and theoretical studies. 2021 , 34, e4138	
610	Rapid and efficient removal of diclofenac sodium from aqueous solution via ternary core-shell CS@PANI@LDH composite: Experimental and adsorption mechanism study. 2021 , 402, 123815	50
609	The synthesis and modification of highly fluorescent carbon quantum dots for reversible detection of water-soluble phosphonate-1-hydroxyethane-1,1-diphosphonic acid by fluorescence spectroscopy. 2021 , 36, 200-209	0
608	Gold at crossroads of radical generation and scavenging at density functional theory level: Nitrogen and oxygen free radicals versus their precursors in the face of nanogold. 2021 , 34,	1
607	Understanding structural and molecular properties of complexes of nucleobases and Au13 golden nanocluster by DFT calculations and DFT-MD simulation. 2021 , 11, 435	4
606	The design of anion-Interactions and hydrogen bonds for the recognition of chloride, bromide and nitrate anions. 2021 , 23, 11455-11465	1
605	Non-stoichiometric molybdenum sulfide clusters and their reactions with the hydrogen molecule. 2021 , 23, 347-355	4
604	A novel surface-active monomer decorating a self-floating adsorbent with high pH adaptability for anionic dyes: Estacking. 2021, 321, 114864	1

603	Experimental and Theoretical Studies of Dimers Stabilized by Two Chalcogen Bonds in the Presence of a NIIIN Pnicogen Bond. 2021 , 125, 657-668	7
602	Perspective of structural flexibility on selective inhibition towards CYP1B1 over CYP1A1 by ∃-naphthoflavone analogs. 2021 , 23, 20230-20246	2
601	Adjacent N-® and CNH2 groups highly efficient amphoteric structure for energetic materials resulting from tautomerization proved by crystal engineering. 2021 , 23, 1544-1549	1
600	Computational investigation of the substituent effect in the [2 + 4] DielsAlder cycloaddition reactions of HSi?Si(para-C6H4X) with benzene. 2021 , 68, 806-816	3
599	Selective Separation of HNO and HCl by Extraction: The Investigation on the Noncovalent Interaction between Extractants and Acids by Density Functional Theory. 2021 , 125, 1214-1226	2
598	From helices to superhelices: hierarchical assembly of homochiral van der Waals 1D coordination polymers. 2021 , 12, 12619-12630	2
597	Solvent effect on xylose-to-furfural reaction in biphasic systems: combined experiments with theoretical calculations.	6
596	Polycentric binding in complexes of trimethylamineoxide with dihalogens 2021 , 11, 6131-6145	О
595	Probing the anomeric effect and mechanism of isomerization of oxazinane rings by DFT methods. 2021 , 19, 1066-1082	0
594	The effect of asymmetric external reorganization energy on electron and hole transport in organic semiconductors. 2021 , 23, 15236-15244	1
593	Boosting intermolecular interactions of fused cyclic explosives: the way to thermostable and insensitive energetic materials with high density. 2021 , 45, 9358-9367	1
592	Extraction and separation of Pd(II)/Pt(IV) by neutral sulfur-containing extractant from hydrochloric acid medium.	o
591	Mechanistic insight into the roles of anions and cations in the degradation of poly(ethylene terephthalate) catalyzed by ionic liquids. 2021 , 23, 18659-18668	2
590	Enhanced Solubility and Antitumor Activity of Curcumin via Breaking and Rebuilding of the Hydrogen Bond. 2021 , 4, 918-927	5
589	Enantioseparation of 5,5'-Dibromo-2,2'-Dichloro-3-Selanyl-4,4'-Bipyridines on Polysaccharide-Based Chiral Stationary Phases: Exploring Chalcogen Bonds in Liquid-Phase Chromatography. 2021 , 26,	6
588	A study on the rules of ligands in highly efficient Rullmide/AC catalysts for acetylene hydrochlorination.	2
587	Effects of lateral-chain thiophene fluorination on morphology and charge transport of BDT-T based small molecule donors: a study with multiscale simulations.	0
586	Synergistic Interplay between Asymmetric Backbone Conformation, Molecular Aggregation, and Charge-Carrier Dynamics in Fused-Ring Electron Acceptor-Based Bulk Heterojunction Solar Cells. 2021 , 13, 2961-2970	4

(2021-2021)

585	Pyromellitic-Based Low Molecular Weight Gelators and Computational Studies of Intermolecular Interactions: A Potential Additive for Lubricant. 2021 , 37, 2954-2962	7
584	The Adsorption Mechanism of Montmorillonite for Different Tetracycline Species at Different pH Conditions: the Novel Visual Analysis of Intermolecular Interactions. 2021 , 232, 1	3
583	Responsive Zwitterionic Polymers with Humidity and Voltage Dual-Switching for Multilevel Date Encryption and Anticounterfeiting. 2021 , 33, 1477-1488	4
582	Electron-Donating C-NH Link Backbone for Highly Alkaline and Mechanical Stable Anion Exchange Membranes. 2021 , 13, 10490-10499	3
581	AlCl3-catalyzed C-H p hosphination of benzene: A mechanistic study. 2021 , 611, 117943	5
580	Theoretical Study of the Structure and Property of Ionic Liquids as Corrosion Inhibitor.	2
579	3,4-Methylenedioxypyrovalerone (MDPV) Sensing Based on Electropolymerized Molecularly Imprinted Polymers on Silver Nanoparticles and Carboxylated Multi-Walled Carbon Nanotubes. 2021 , 11,	2
578	Constructing Donor-Resonance-Donor Molecules for Acceptor-Free Bipolar Organic Semiconductors. 2021 , 2021, 1-10	O
577	Synthesis, structural and computational studies of new tetrazole derivatives. 2021 , 1226, 129341	5
576	New evidence on non-covalent interactions in crystalline halo-substituted boron difluoride acetylacetonates from vibrational spectra, model calculations and visualization program tools. 2021 , 1227, 129532	1
575	Computational Exploration of Ambiphilic Reactivity of Azides and Sustmann's Paradigmatic Parabola. 2021 , 86, 5792-5804	4
574	Reversible Addition of Carbon Dioxide to Main Group Metal Complexes at Temperatures about 0 LC. 2021 , 27, 5745-5753	8
573	The interaction and mechanism between threonine-montmorillonite composite and Pb2+ or Cu2+: Experimental study and theory calculation. 2021 , 326, 115243	3
572	Self-Assembled Copper Nanoclusters for Electrocatalytic Glucose Oxidation. 2021 , 4, 4129-4139	2
571	Homogenous Liquid[Liquid Extraction of Au(III) from Acidic Medium by Ionic Liquid Thermomorphic Systems. 2021 , 9, 4894-4902	6
570	Ni/Cu-catalyzed silylation of allylic alcohol: Theoretical studies on the mechanisms, regioselectivity, and role of ligand. 2021 , 504, 111456	
569	Stereoelectronic effects in stabilizing protein-N-glycan interactions revealed by experiment and machine learning. 2021 , 13, 480-487	3
568	Bi-functional hydrogen and coordination bonding surfactant: A novel and promising collector for improving the separation of calcium minerals. 2021 , 585, 787-799	12

567	Competition between Inter and Intramolecular Tetrel Bonds: Theoretical Studies Complemented by CSD Survey. 2021 , 22, 924-934	2
566	Screening Ionic Liquids Based on Ionic Volume and Electrostatic Potential Analyses. 2021 , 125, 3653-3664	9
565	Interfacial Carrier-Transfer Channel Optimization Based on Hydrogen Bonds for High-Performance Organic Solar Cells. 2021 , 4, 3881-3890	2
564	Rational design of [bridge to forecast photoelectric performance of dye. 2021 , 29, 045007	O
563	Enantioseparations of polyhalogenated 4,4'-bipyridines on polysaccharide-based chiral stationary phases and molecular dynamics simulations of selector-selectand interactions. 2021 , 42, 1853-1863	3
562	Unraveling the Mechanism of Near-Infrared Thermally Activated Delayed Fluorescence of TPA-Based Molecules: Effect of Hydrogen Bond Steric Hindrance. 2021 , 125, 2905-2912	2
561	Crystallographic and Theoretical Evidences of Anion???Anion Interaction. 2021, 22, 818-821	10
560	The adsorption performance and micro-mechanism of MoS/montmorillonite composite to atenolol and acebutolol: Adsorption experiments and a novel visual study of interaction. 2021 , 213, 111993	5
559	Iodine-Substituted Lithium/Sodium -Decaborates: Syntheses, Characterization, and Solid-State Ionic Conductivity. 2021 , 13, 17554-17564	11
558	Anion-Anion Interactions in Aerogen-Bonded Complexes. Influence of Solvent Environment. 2021 , 26,	6
557	Highly stable electron-withdrawing C O link-free backbone with branched cationic side chain as anion exchange membrane. 2021 , 624, 119052	5
556	A Computational Mechanistic Analysis of Iridium-Catalyzed C(sp3) Borylation Reveals a One-Stone wo-Birds Strategy to Enhance Catalytic Activity. 2021 , 11, 4833-4847	3
555	Electrostatic Balance Parameter Mediated Energy Functions-Toward the Stability and Performance of Explosives. 2021 , 46, 1313-1323	1
554	Azabuckybowl-based molecular pincers of fullerenes: A noncovalent intermolecular D-A-D system. 2021 , 114, 108293	1
553	Insights into interfacial interaction mechanism of dyes sorption on a novel hydrochar: Experimental and DFT study. 2021 , 233, 116432	11
552	Solubility Behavior of CO in Ionic Liquids Based on Ionic Polarity Index Analyses. 2021 , 125, 3665-3676	9
551	Comparative study of the hydrogen bonding properties between bis(fluorosulfonyl)imide/bis(trifluoromethyl)sulfonylimide-based ether-functionalized ionic liquids and methanol. 2021 , 328, 115333	5
550	Side-chain manipulation of poly (phenylene oxide) based anion exchange membrane: Alkoxyl extender integrated with flexible spacer. 2021 , 624, 119088	17

549	Co-amorphization Story of Furosemide-Amino Acid Systems: Protonation and Aromatic Stacking Insights for Promoting Compatibility and Stability. 2021 , 21, 3280-3289	0
548	High regioselectivity in the amination reaction of isoquinolinequinone derivatives using conceptual DFT and NCI analysis. <i>Journal of Molecular Graphics and Modelling</i> , 2021 , 104, 107828	2
547	The theoretical investigation on properties of paeonol and its isomers. 2021 , 119, e1925363	3
546	Ni2P Nanosheets: A High Catalytic Activity Platform for Electrochemical Detection of Acetaminophen. 2021 , 39, 1849-1854	5
545	Unveiling the Reaction Mechanism of the Das/Chechik/Marek Synthesis of Stereodefined Quaternary Carbon Centers. 2021 , 11, 5002	
544	Cocrystals of Oxymatrine: Reducing Hygroscopicity and Affecting the Dissolution Rate. 2021 , 21, 3874-3888	Ο
543	Theoretical insights into the dimerization mechanism of aluminum species at two different pH conditions. 2021 , 520, 120311	1
542	Co (II) and Cd (II) complexes with imidazole-2-carboxaldehyde groups: spectroscopic, antibacterial, Hirshfeld surfaces analyses, and TD/DFT calculations. 2021 , 35, e6279	3
541	Theoretical research of covalent and controllable molecular brake based on 9-triptycene. 2021 , 140, 1	
540	Comparative Structural Study of Three Tetrahalophthalic Anhydrides: Recognition of XIIIO (anhydride) Halogen Bond and BIIIO (anhydride) Interaction. 2021 , 26,	1
539	Interaction between carboplatin with B12P12 and Al12P12 nano-clusters: A computational investigation. 2021 , 196, 751-759	1
538	Complex formation of titanocene dichloride anticancer and Al12N12 nano-cluster: A quantum chemical investigation of solvent, temperature and pressure effects. 2021 , 20, 19-32	2
537	Using Quantum Density Functional Theory Methods to Study the Adsorption of Fluorouracil Drug on Pristine and Al, Ga, P and As Doped Boron Nitride Nanosheets. 2021 , 6, 6119-6131	2
536	Facile Fabrication of Functionalized Separators for Lithium-Ion Batteries with Ionic Conduction Path Modifications via the Ray Co-irradiation Grafting Process. 2021 , 13, 27663-27673	3
535	Density Prediction of Ionic Liquids at Different Temperatures Using the Average Free Volume Model. 2021 , 6, 14869-14874	О
534	New deep eutectic solvent based superparamagnetic nanofluid for determination of perfluoroalkyl substances in edible oils. 2021 , 228, 122214	5
533	A computational toolbox for molecular property prediction based on quantum mechanics and quantitative structure-property relationship. 1	0
532	Distinct roles of Ag(I) and Cu(II) as cocatalysts in the intramolecular cyclization of N-methyl-N-phenylanthranilic acid: A theoretical investigation. 2021 , 509, 111634	

531	Mo Fischer Carbene Complexes: A DFT Study on the Prediction of Redox Potentials.	3
530	Analysis and comparison of metal-doped on Graphene-Genistein using QM/MM calculations.	О
529	Density functional theory B ased investigation of CaO/char catalyzing the transformation of NH3 to N2. 2021 , 156, 105124	1
528	Cocrystallization Enabling Photoinduced Rotation of an Azopyridine Crystal. 2021 , 21, 3936-3946	3
527	Perspective of Zn3O3 ring cluster via density functional theory. 2021 , 27, 102343	1
526	Quantum chemical, spectroscopic investigations, molecular docking and cytotoxic evaluation of 1-Methyl-indole-3-carboxaldehyde. 2021 , 33, 100698	1
525	Insights into complexation and enantioselectivity of uranyl-2-(2-hydroxy-3-methoxyphenyl)-9-(2-hydroxyphenyl)thiopyrano[3,2-h]thiochromene-4,7-dione with R/S-organophosphorus pesticides. 2021 , 35, e6331	О
524	Investigation of the assembly mechanism of N1, N4-di (pyridin-4-yl) terephthalamide with pillar[5]arene: Experiment and quantum chemical study. 2021 , 772, 138533	1
523	A study of cation-dependent inverse hydrogen bonds and magnetic exchange-couplings in lanthanacarborane complexes. 2021 , 24, 102760	1
522	SolventAntisolvent Competitive Interactions Mediate Imidacloprid Polymorphs in Antisolvent Crystallization. 2021 , 21, 4318-4328	2
521	The interaction between carboplatin anticancer drug and B12N12 nano-cluster: A computational investigation. 2021 , 1-10	3
520	Antimicrobial activities of cadmium (II) and nickel (II) complexes containing pyridine ring: Investigation of crystallographic, spectroscopic, Hirshfeld surface analysis, and TD/DFT calculations. 2021 , 35, e6360	1
519	Molecular thermodynamic and dynamic insights into gas dehydration with imidazoliumBased ionic liquids. 2021 , 416, 129168	10
518	Phosphorus Deficiency Promoted Hydrolysis of Organophosphate Esters in Plants: Mechanisms and Transformation Pathways. 2021 , 55, 9895-9904	3
517	5-Substituted isatin thiosemicarbazones as inhibitors of tyrosinase: Insights of substituent effects. 2021 , 255, 119669	2
516	Effect of electric field strength on deformation and breakup behaviors of droplet in oil phase: A molecular dynamics study. 2021 , 333, 115995	9
515	Aggregation Behavior of Asphalt on the Natural Gas Hydrate Surface with Different Surfactant Coverages. 2021 , 125, 16378-16390	9
514	Theoretical calculation on the interaction mechanism between 2,6-diamino-3,5-dinitropyrazine-1-oxide and ammonium perchlorate. 1-17	О

513	Terpenoid-capric acid based natural deep eutectic solvent: Insight into the nature of low viscosity. 2021 , 3, 100116	5
512	SepPCNET: Deeping Learning on a 3D Surface Electrostatic Potential Point Cloud for Enhanced Toxicity Classification and Its Application to Suspected Environmental Estrogens. 2021 , 55, 9958-9967	5
511	Influence of Fluorine Substitution on Nonbonding Interactions in Selected Para-Halogeno Anilines. 2021 , 22, 2115-2127	2
510	Probing nano-QSAR to assess the interactions between carbon nanoparticles and a SARS-CoV-2 RNA fragment. 2021 , 219, 112357	4
509	DFT study of chemical reactivity parameters of lithium polysulfide molecules Li2Sn(1🛭 B) in gas and solvent phase. 2021 , 1202, 113323	3
508	Catalytic S Ar Hydroxylation and Alkoxylation of Aryl Fluorides. 2021 , 60, 20391-20399	4
507	High performance task-specific ionic liquid in uranium extraction endowed with negatively charged effect. 2021 , 336, 116601	1
506	Tuning the activity of known drugs via the introduction of halogen atoms, a case study of SERT ligands - Fluoxetine and fluvoxamine. 2021 , 220, 113533	3
505	Double-Regiodetermining-Stages Mechanistic Model Explaining the Regioselectivity of Pd-Catalyzed Hydroaminocarbonylation of Alkenes with Carbon Monoxide and Ammonium Chloride. 2021 , 86, 12988-13000	1
504	Group 14 Central Atoms and Halogen Bonding in Different Dielectric Environments: How Germanium Outperforms Silicon. 2021 , 86, 1387-1396	
503	Comprehensive investigations of interaction properties of polylactic Acid-Attapulgite composite by reactive molecular dynamics simulations and dispersion corrected DFT calculations. 2021 , 28, 78-86	Ο
502	Catalytic SNAr Hydroxylation and Alkoxylation of Aryl Fluorides. 2021 , 133, 20554-20562	1
501	Facile access to highly flexible and mesoporous structured silica fibrous membranes for tetracyclines removal. 2021 , 417, 129211	12
500	Fine-diameter SiBITN ceramic fibers enabled by polyborosilazanes with Nthethyl pendant group. 2021 , 41, 5016-5025	O
499	Computational investigation, comparative approaches, molecular structural, vibrational spectral, non-covalent interaction (NCI), and electron excitations analysis of benzodiazepine derivatives. 2021 , 27, 266	5
498	Isomerization energies and surface electrostatic potential analyses on nitriles and isocyanides. 2021 , 27, 257	O
497	Study of the Redox Potentials of Benzoquinone and Its Derivatives by Combining Electrochemistry and Computational Chemistry. 2021 , 98, 3019-3025	2
496	Modeling the DFT structural and reactivity studies of a pyrimidine -6-carboxylate derivative with reference to its wavefunction-dependent, MD simulations and evaluation for potential antimicrobial activity. 2021 , 1237, 130397	10

495	Nitrogen-Doped Buckybowls as Potential Scaffold Material for Lithium-Sulfur Battery: A DFT Study. 2021 , 12, 678	1
494	Structural and vibrational spectral investigation on the identification of Non-Linear Optical properties and wave function analyses (electrostatic potential, electron localisation function, localised orbital locator) of 3-Ethoxy Salicilaldehyde. 2021 , 47, 1217-1233	2
493	Kinetics and mechanisms of phenolic compounds by Ferrate(VI) assisted with density functional theory. 2021 , 415, 125563	12
492	Closer look into the structures of tetrabutylammonium bromideglycerol-based deep eutectic solvents and their mixtures with water. 2021 , 338, 116676	1
491	Achieve 100% transmission via grafting hydroxyl groups on CNT nanomotors. 2021 , 29, 59-65	0
490	Theoretical study on pentiptycene molecular brake: photoinduced isomerization and photoinduced electron transfer. 2021 , 27, 289	
489	Ultrasound-assisted theophylline polymorphic transformation: Selective polymorph nucleation, molecular mechanism and kinetics analysis. 2021 , 77, 105675	1
488	Metal-Involving Chalcogen Bond. The Case of Platinum(II) Interaction with Se/Te-Based EHole Donors. 2021 , 143, 15701-15710	9
487	Solubility and thermodynamic properties of flonicamid in pure and binary solvents in the temperature range of 283.15B23.15IK. 2021 , 337, 116233	4
486	Pnictogen effects on the electronic interactions in the Lewis pair complexes Ph3EB(C6F5)3 (E⊞P, As, Sb). 2021 , 949, 121944	2
485	Insights into the photocatalytic peroxymonosulfate activation over defective boron-doped carbon nitride for efficient pollutants degradation. 2021 , 418, 126338	4
484	Possible coordination modes of copper(II) atom in model silsesquioxanes complexes at various pH conditions: DFT study. 2021 , 778, 138739	1
483	Synthesis and properties of symmetric glycerol-derived 1,2,3-triethers and 1,3-diether-2-ketones for CO2 absorption. 2021 , 248, 117150	2
482	Probing Limits of a C=C Bond Activation by N-Coordinated Organopnictogen(I) Compounds. 2021 , 2021, 4030	2
481	Quantum Chemical Calculation of the Effects of HO on Oxygen Functional Groups during Coal Spontaneous Combustion. 2021 , 6, 25594-25607	2
480	Nano zero valent iron encapsulated in graphene oxide for reducing uranium. 2021 , 278, 130229	8
479	Computational study of the electrostatic potential and charges of multivalent ionic liquid molecules. 2021 , 340, 117190	2
478	Separation of lithium isotopes by crown ether-room temperature ionic liquid-anisole friendly solvent system. 2021 , 340, 117207	Ο

477	Experimental and theoretical study on the adsorption mechanism of Amino trimethylphosphate (ATMP) functionalized hydroxyapatite on Pb (II) and Cd (II). 2021 , 626, 127029	6
476	Crystal structure and optical property of a Cadmium(II) complex based on triphenylamine derivative Theoretical and experimental investigation. 2021 , 238, 118270	Ο
475	Selective determination of epinephrine using electrochemical sensor based on ordered mesoporous carbon / nickel oxide nanocomposite. 2021 , 233, 122545	12
474	Peroxymonosulfate activation through 2D/2D Z-scheme CoAl-LDH/BiOBr photocatalyst under visible light for ciprofloxacin degradation. 2021 , 420, 126613	24
473	Adsorption of alkali and alkaline earth ions on nanocages using density functional theory. 2021 , 1204, 113391	8
472	Insight into Anticorrosion Mechanism of Ampicillin on Mild Steel in Acidic Environment: A Combined Experimental and Theoretical Approach. 2021 , 2021, 1-12	
47 ¹	Revisiting UF6, NpF6 and PuF6 for bonding and molecular surface analysis within density functional theory: Comparative study at the different theory levels with the same basis set. 2021 , 209, 115452	
470	A novel ion-pair strategy for efficient separation of lithium isotopes using crown ethers. 2021 , 274, 118989	3
469	Understanding the conformational, electronic and vibrational properties of Tetrahydrocannabinol (THC) and Cannabidiol (CBD). Pharmacophoric similarities and differences. 2021 , 1244, 130945	4
468	Reactivity properties and adsorption behavior of a triazole derivative IDFT and MD simulation studies. 2021 , 341, 117439	6
467	Thiazolium-based ionic liquids: Synthesis, characterization and physicochemical properties. 2021 , 342, 117553	O
466	Predicting both lower and upper flammability limits for fuel mixtures from molecular structures with same descriptors. 2021 , 155, 177-183	O
465	The highly specific detection and mechanism of Cu-MOF-74 fluorescent probe to amino trimethylene phosphonic acid: Experimental study and theoretical calculation of quantum chemistry. 2021 , 341, 117442	O
464	Hierarchical sheet triply periodic minimal surface lattices: Design, geometric and mechanical performance. 2021 , 209, 109931	3
463	Enhancing the reactivity of carbon-nanotube for carbon monoxide detection by mono- and co-doping of boron and nitrogen heteroatoms: A DFT and TD-DFT study. 2021 , 158, 110230	2
462	Metal-free Fenton-like photocatalysts based on covalent organic frameworks. 2021 , 298, 120548	9
461	Crystallographic, spectroscopic, TD/DFT calculations and Hirshfeld surface analysis of cadmium(II) coordination polymer containing pyridine ring. 2021 , 1245, 131028	5
460	Adsorption of acetone onto the pristine and Al-doped ZnO nanotubes: A dispersion corrected DFT study. 2021 , 136, 106141	O

459	Amidoxime modified chitosan/graphene oxide composite for efficient adsorption of U(VI) from aqueous solutions. 2021 , 9, 106363	2
458	Explore fused-ring core incorporated A-ED-EA type acceptors and their application in organic solar cells: Insight into molecular conformation, optical and electrochemical properties, film morphology, and energy loss. 2021 , 196, 109572	
457	Exploring the antibacterial activity of 1, 2 diaminoethane hexanedionic acid by spectroscopic, electronic, ELF, LOL, RDG analysis and molecular docking studies using DFT method. 2022 , 1247, 131388	4
456	Molecular structure and DFT calculations of aqua(5,10,15,20-tetrakis[4-(benzoyloxy)phenyl] porphyrinato)magnesium-dioxane. 2022 , 1248, 131469	O
455	Co-degradation of coexisting pollutants methylparaben (mediators) and amlodipine in enzyme-mediator systems: Insight into the mediating mechanism. 2022 , 423, 127112	3
454	Three-dimension hierarchical composite via in-situ growth of Zn/Al layered double hydroxide plates onto polyaniline-wrapped carbon sphere for efficient naproxen removal. 2022 , 423, 127192	10
453	Understanding the fundamental interaction mechanism of hazardous gases and imidazolium based ionic liquids for efficient gas adsorption. 2022 , 247, 117031	2
452	How to enhance the regenerability of biphasic absorbents for CO2 capture: An efficient strategy by organic alcohols activator. 2022 , 429, 132264	2
451	Imino-bridged N-rich energetic materials: C4H3N17 and their derivatives assembled from the powerful combination of four tetrazoles. 2021 , 23, 5377-5384	1
450	Chalcogen bonding interactions in chelating, chiral bis(selenocyanates). 2021 , 45, 76-84	4
449	Deep eutectic solvent-based green absorbents for the effective removal of volatile organochlorine compounds from biogas. 2021 , 23, 4814-4827	8
448	Efficient evaluation of electrostatic potential with computerized optimized code. 2021 , 23, 20323-20328	75
447	Anion-anion and anion-neutral triel bonds. 2021 , 23, 4818-4828	11
446	Orientation effects on C2(5)-C2?(5?) linked bioxazole isomers synthesized via regioselective and sequential C H arylation. 2021 , 32, 425-428	O
445	Insights into the nucleophilic substitution of pyridine at an unsaturated carbon center 2021 , 11, 24238-2424	16 O
444	Solvation effect on the ESIPT mechanism of nitrile-substituted -hydroxy-2-phenyl-oxazolines 2021 , 11, 25795-25800	3
443	Surface modification of polyamide reverse osmosis membranes with small-molecule zwitterions for enhanced fouling resistance: a molecular simulation study. 2021 , 23, 6623-6631	2
442	Theoretical insight into dihydrogen activation with Ediketiminato ligand supported Group 13 and 14 elements: mechanism and activity difference. 2021 , 45, 14789-14796	

441	Anionanion (MX) dimers (M = Zn, Cd, Hg; X = Cl, Br, I) in different environments. 2021 , 23, 13853-13861	6
440	Construction of a Z-scheme 1D/2D FeV3O8/g-C3N4 composite for ibuprofen degradation: mechanism insight, theoretical calculation and degradation pathway. 2021 , 11, 3466-3480	8
439	Efficient and organic host-guest room-temperature phosphorescence: tunable triplet-singlet crossing and theoretical calculations for molecular packing. 2021 , 12, 6518-6525	34
438	The physical nature of the interaction in DMSO extraction separation of CH isomer/-decane systems. 2021 , 23, 22629-22639	O
437	Extending the Marcus Escale of Solvent Softness Using Conceptual Density Functional Theory and the Orbital Overlap Distance: Method and Application to Ionic Liquids. 2020 , 49, 614-628	1
436	Experimental and computational approach on p-toluenesulfonamide and its derivatives. 2020 , 1218, 128503	2
435	Halogen Bonding Involving Palladium(II) as an XB Acceptor. 2021 , 21, 1159-1177	11
434	Self-assembled ionic nanofibers derived from amino acids for high-performance particulate matter removal. 2019 , 7, 4619-4625	28
433	Extensive removal of thallium by graphene oxide functionalized with aza-crown ether 2020, 10, 44470-444	80 5
432	Consistency and variability of cocrystals containing positional isomers: the self-assembly evolution mechanism of supramolecular synthons of cresol-piperazine. 2019 , 6, 1064-1073	7
431	QUANTUM-CHEMICAL INVESTIGATION OF THE COMPLEXATION OF TITANOCENE DICHLORIDE WITH C20 AND M+@C20 (M+ = Li, Na, K) CAGES. 2020 , 61, 1681-1690	1
430	Modified mesoporous Y zeolite catalyzed nitration of azobenzene using NO2 as the nitro source combined with density functional theory studies.	O
429	Correlations between the ECD spectra and absolute configuration of bridged-ring lactones: revisiting Beecham's rule. 2021 , 19, 9266-9275	0
428	Two mono- and dinuclear Cu (II) complexes derived from 3-ethoxy salicylaldehyde: X-ray structures, spectroscopic, electrochemical, antibacterial activities, Hirshfeld surfaces analyses, and time-dependent density functional theory studies. e6475	O
427	Efficient improvement of W05-based dyes by inserting auxiliary electron acceptors for dye-sensitized solar cells: A theoretical investigation. e4290	
426	Energetic Windmill: Computational insight into guanidine-based nitroazole-substituted compounds as energetic materials. 2021 , 1206, 113485	
425	Computational chemistry methods for modelling non-covalent interactions and chemical reactivity[An overview. 2021 , 98, 100208	4
424	Theoretical study on mechanism of decomposition reaction of 1,2,4-triazole derivatives.	

423	Microscopic Reaction Mechanisms of Formic Acid Generated During Pyrolysis of Cellulosic Insulating Paper. 2021 , 28, 1661-1668	4
422	Energetic and Geometric Characteristics of the Substituents: Part 2: The Case of NO, Cl, and NH Groups in Their Mono-Substituted Derivatives of Simple Nitrogen Heterocycles. 2021 , 26,	1
421	The Theoretical Investigation of Monohydroxy Flavone:A combined DFT and Molecular Docking Study. 2021 , 131823	1
420	Quantum-chemical calculations on the slippage of cyclopentadienyl and indenyl ligands in the (B-dienyl)Ir(PX3)3; (X = H, F, Cl, Me) complexes. 2021 , 68, 785-792	
419	Facile immobilization of ethylenediamine tetramethylene-phosphonic acid into UiO-66 for toxic divalent heavy metal ions removal: An experimental and theoretical exploration. 2022 , 806, 150652	8
418	Study on the reaction mechanism of CH2O + NO2 transformed by PbO/SnO in double-base propellants through theoretical calculation and experiment. 2022 , 236, 111768	1
417	Experimental and theoretical calculations study on heterogeneous reduction of NO by char/NH3 in the reduction zone of ammonia co-firing with pulverized coal: Influence of mineral Fe. 2022 , 310, 122374	2
416	Insights into the interaction between NO and char(N) containing different functional forms: Mechanistic, thermodynamic and kinetic studies. 2022 , 237, 111823	3
415	Triel bonds within anionanion complexes. 2021 , 23, 25097-25106	1
414	(4n +2)[Huckel rule of Bn NnC(8-2n) H8 as anti-cancer heterocyclic systems. 2020, 11, 129-150	
414	(4n +2)[Huckel\(\text{I rule of Bn NnC(8-2n) H8 as anti-cancer heterocyclic systems. 2020, 11, 129-150}\) Substituente en isomeriese effekte op die reduksieen oksidasiepotensiaal van tris(\(\text{Ediketonato} \)) mangaan(\(\text{III} \)) komplekse: DFT en MESP analises. 2020, 119-133	
	Substituente en isomeriese effekte op die reduksieen oksidasiepotensiaal van tris(Ediketonato)	5
413	Substituente en isomeriese effekte op die reduksieen oksidasiepotensiaal van tris(Ediketonato) mangaan(III) komplekse: DFT en MESP analises. 2020 , 119-133 How do molecular interactions affect fluorescence behavior of AIEgens in solution and aggregate	5
413 412	Substituente en isomeriese effekte op die reduksieen oksidasiepotensiaal van tris(Ediketonato) mangaan(III) komplekse: DFT en MESP analises. 2020, 119-133 How do molecular interactions affect fluorescence behavior of AIEgens in solution and aggregate states?. 2022, 65, 135 New Energetic Metal-Organic Framework (E-MOF) based on a sodium(I)-containing energetic metal	5
413 412 411	Substituente en isomeriese effekte op die reduksieen oksidasiepotensiaal van tris(Ediketonato) mangaan(III) komplekse: DFT en MESP analises. 2020, 119-133 How do molecular interactions affect fluorescence behavior of AIEgens in solution and aggregate states?. 2022, 65, 135 New Energetic Metal-Organic Framework (E-MOF) based on a sodium(I)-containing energetic metal salt incorporating guanidinium ions.	
413 412 411 410	Substituente en isomeriese effekte op die reduksieen oksidasiepotensiaal van tris(Ediketonato) mangaan(III) komplekse: DFT en MESP analises. 2020, 119-133 How do molecular interactions affect fluorescence behavior of AIEgens in solution and aggregate states?. 2022, 65, 135 New Energetic Metal-Organic Framework (E-MOF) based on a sodium(I)-containing energetic metal salt incorporating guanidinium ions. Exploring GuestHost Interactions in Gas Hydrates: Insights from Quantum Mechanics. Quantum Chemistry Calculation Study on Chain Reaction Mechanisms and Thermodynamic	O
413 412 411 410 409	Substituente en isomeriese effekte op die reduksieen oksidasiepotensiaal van tris(Ediketonato) mangaan(III) komplekse: DFT en MESP analises. 2020, 119-133 How do molecular interactions affect fluorescence behavior of AIEgens in solution and aggregate states?. 2022, 65, 135 New Energetic Metal-Organic Framework (E-MOF) based on a sodium(I)-containing energetic metal salt incorporating guanidinium ions. Exploring GuestBlost Interactions in Gas Hydrates: Insights from Quantum Mechanics. Quantum Chemistry Calculation Study on Chain Reaction Mechanisms and Thermodynamic Characteristics of Coal Spontaneous Combustion at Low Temperatures. 2021, 6, 30841-30855	0

405	The theoretical investigation of the opto-electronic properties of designed molecules having 2-(2-Methylene-3-oxo-indane-1-ylidene)malononitrile as end-capped acceptors. 2020 ,	
404	Synthesis, crystal structure, Hirshfeld surface analysis, MEP study and mol-ecular docking of -{3-[(4-meth-oxy-phen-yl)carbamo-yl]phen-yl}-3-nitro-benzamide as a promising inhibitor of hfXa. 2020 , 76, 1762-1767	1
403	ANALYSIS OF LOCALIZED ORBITALS IN AZABORA DERIVATIVES OF [8] ANNULENE: IN THE VIEWPOINT OF AROMATICITY AND INDUCED RING CURRENTS. 2020 , 61, 1551-1567	O
402	Neutral nickel(II) complex bearing hemilabile N,S-donor ligands ßtructural, Hirshfeld surfaces and DFT studies. 2020 , 709, 98-110	2
401	New perspectives on the laser initiation for metal tetrazine complexes: a theoretical study. 2021,	O
400	Understanding gas absorption in multivalent ionic liquids via solute-solvent interaction analyses. 2022 , 786, 139204	1
399	Determination of dopamine based on a temperature-sensitive PMEOMA and Au@rGO-MWCNT nanocomposite-modified electrode 2021 ,	2
398	SUBSTITUENT EFFECT IN [2+4] DIELSALDER CYCLOADDITION REACTIONS OF ANTHRACENE WITH C2X2 (X = H, F, Cl, Me): A COMPUTATIONAL INVESTIGATION. 2021 , 62, 1551-1562	1
397	Dispersion-corrected DFT investigations on the interaction of glycine amino acid with metal organic framework MOF-5. 2021 , 626, 413446	4
396	Quantitative tuning of ionic metal species for ultra-selective metal solvent extraction toward high-purity vanadium products. 2021 , 425, 127756	1
395	On the Ability of Nitrogen to Serve as an Electron Acceptor in a Pnicogen Bond. 2021 , 125, 10419-10427	4
394	Probing into the Outcome of Charge Transfer Interactions and Hyperconjugative Effect on the Antibacterial Molecule 4-Dimethylaminopyridine using Spectroscopic Elucidations and DFT Calculations. 2021 , 132059	1
393	Being positive is not everything - experimental and computational studies on the selectivity of a self-assembled, multiple redox-state, receptor that binds anions with up to picomolar affinities. 2021 ,	O
392	Reconsidering the Roles of Noncovalent Intramolecular 🏻 Docks 🖟 EConjugated Molecules.	2
391	Effects of Different Parameter Settings for 3D Data Smoothing and Mesh Simplification on Near Real-Time 3D Reconstruction of High Resolution Bioceramic Bone Void Filling Medical Images. 2021 , 21,	О
390	An all-in-one approach for synthesis and functionalization of nano colloidal gold with acetylacetone. 2021 , 33,	
389	Biotinylation as a tool to enhance the uptake of small molecules in Gram-negative bacteria. 2021 , 16, e0260023	0
388	Stable Long Cycling of Small Molecular Organic Acid Electrode Materials Enabled by Nonflammable Eutectic Electrolyte. 2021 , e2104538	2

387	Glycerol-derived solvents containing two or three distinct functional groups enabled by trifluoroethyl glycidyl ether. e17533	1
386	Separation and Recovery of Iridium(IV) from a Simulated Secondary Resource Leachate by Extraction - Electrodeposition.	
385	Graphene Oxide (Ferrocenylmethyl) Dimethylammonium Nitrate Composites as Catalysts for Ammonium Perchlorate Thermolysis.	4
384	High-Efficiency Non-Fullerene Acceptors Developed by Machine Learning and Quantum Chemistry 2022 , e2104742	6
383	Roles of hydrogen bond and ion bridge in adsorption of two bisphenols onto montmorillonite: an experimental and DFT study. 2022 , 217, 106406	1
382	Interaction of halomethane CH3Z ($Z = F$, Cl, Br) with X12Y12 ($X = B$, Al, Ga & $Y = N$, P, As) nanocages. 2022 , 1208, 113544	2
381	Stable alkoxy chain enhanced anion exchange membrane and its fuel cell. 2022 , 644, 120179	1
380	Efficient detection for Nitrofurazone based on novel AgS QDs/g-CN fluorescent probe 2021 , 269, 120727	O
379	Simple reaction to prepare a heat-resistant and insensitive explosive (2-nitro-[1,2,4]triazolo[1,5-a][1,3,5]triazine-5,7-diamine) and its derivatives. 2022 , 432, 134297	2
378	The Bff-onlfluorescent probe based on salicylic acid for rapid and selective detection of 1-hydroxyethane-1,1-diphosphonic acid. 2022 , 426, 113740	
377	Synergistic strongly coupled super-deamidation of wheat gluten by glucose-organic acid natural deep eutectic solvent and the efficaciousness of structure and functionality. 2022 , 125, 107437	O
376	One-Step construction of Polyimide/NH-UiO-66 heterojunction for enhanced photocatalytic degradation of sulfonamides 2022 , 612, 536-549	O
375	A Simulation Research on Diffusion Processes of Discharging Decomposition Products of C4F7N/CO2 in Gas Insulated Transmission Lines. 2020 ,	
374	Incorporating Amino Acids Functionalized Graphene Oxide Nanosheets into Pebax Membranes for CO 2 Separation.	
373	Exploring of the Solvent Effect on the Electronic Structure and 14N NMR Chemical Shift of Cyclic-N3S3Cl3: A Computational Investigation. 2021 , 15, S14-S21	1
372	EDA, CDA and QTAIM Investigations in the (para-C5H4X) Ir(PH3)3 Iridabenzene Complexes. 2021 , 15, S6-S13	O
371	Safe and Stable Lithium Metal Batteries Enabled by an Amide-Based Electrolyte 2022 , 14, 44	8
370	Palladium Nanoparticle-Modified Carbon Spheres @ Molybdenum Disulfide Core-Shell Composite for Electrochemically Detecting Quercetin. 2022 , 10, 56	O

369	Comparative enantioseparation of planar chiral ferrocenes on polysaccharide-based chiral stationary phases 2022 ,	2
368	Deep eutectic solvents boosting solubilization and Se-functionalization of heteropolysaccharide: Multiple hydrogen bonds modulation 2022 , 284, 119159	1
367	Novel zinc (II) and nickel (II) complexes of a quinazoline-based ligand with an imidazole ring: Synthesis, spectroscopic property, antibacterial activities, time-dependent density functional theory calculations and Hirshfeld surface analysis.	0
366	Structure identification and analysis of the suspected chemical precursor of 2-fluorodeschloroketamine and its decomposition products 2022 ,	
365	Exploration of hydrogen-bonded organic framework (HOF) as highly efficient adsorbent for rhodamine B and methyl orange. 2022 , 330, 111624	2
364	Dispersion and Steric Effects on Enantio-/Diastereoselectivities in Synergistic Dual Transition-Metal Catalysis 2022 ,	7
363	Vacuum-assisted and alkali roasting for desulfurization of petroleum coke. 2022, 332, 130052	2
362	Multi-Oxyanion Detection by an Organic Field-Effect Transistor with Pattern Recognition Techniques and Its Application to Quantitative Phosphate Sensing in Human Blood Serum 2022 ,	4
361	Density functional theory study on the reaction mechanism of Ni+-catalysed cyclohexane dehydrogenation. 1	0
360	X-ray structures, spectroscopic, antimicrobial activity, ESP/HSA and TD/DFT calculations of Bi(III) complex containing imidazole ring. 2022 , 1256, 132517	O
359	Synthesis of 1, 3, 5-trisubstituted-4,5-dihydro-1H-pyrazole catalyzed by vitamin B1 and its fluorescence properties.	1
358	Mechanism of heteroatom-doped Cu5 catalysis for hydrogen evolution reaction. 2022 , 47, 7802-7812	1
357	Structural, thermal, vibrational, solubility and DFT studies of a tolbutamide co-amorphous drug delivery system for treatment of diabetes 2022 , 615, 121500	1
356	Computational study of metformin hydrochloride nucleation in hydroxylic solvents: Experimental kinetics and DFT simulation 2022 , 616, 121517	
355	Non-covalent binding interaction between phthalic acid esters and DNA 2022, 161, 107095	1
354	Synthesis of ZIF-67 derived honeycomb porous Co/NC catalyst for AO7 degradation via activation of peroxymonosulfate. 2022 , 286, 120470	1
353	The uptake performance and microscopic mechanism of inorganic-organic phosphorus hybrid amorphous hydroxyapatite for multiple heavy metal ions. 2022 , 640, 128384	0
352	Investigation of the efficient adsorption performance and adsorption mechanism of 3D composite structure La nanosphere-coated Mn/Fe layered double hydrotalcite on phosphate 2022 , 614, 478-488	5

351	Multi-objective optimization and extraction mechanism understanding of ionic liquid assisted in extracting essential oil from Forsythiae fructus. 2022 , 61, 6897-6906	1
350	Exploring interaction modes between polysaccharide-based selectors and biologically active 4,4?-bipyridines by experimental and computational analysis. 2022 , 2, 100030	1
349	Degradation mechanism and eco-toxicity assessment of bisphenol S based on peroxymonosulfate activated with Co3O4 surfaces. 2022 , 341, 130881	0
348	Synthesis of 3,3,3-trifluoropropyne from chlorotrifluoropropene isomers in liquid phase. 2022 , 255-256, 109950	
347	Synthesis, structural, computational, and antiproliferative activity studies of new steroidal tetrazole derivatives. 2022 , 1256, 132577	O
346	Charge scaling parameter evaluation for multivalent ionic liquids with fixed point charge force fields. 2022 , 2, 100020	1
345	Experimental and computational tuning of metalla-N-heterocyclic carbenes at palladium(II) and platinum(II) centers 2022 ,	1
344	Synthesis of Au/Ni2p Nanosheet Arrays with Porous Grids as a High-Performance Electrode for the Determination of Hydroquinone in Domestic Sewage.	
343	Breaking Through the Separation Barrier of Zr(IV) and Hf(IV): The Magical Effect of Bisamide Ligand.	
342	Computational and Experimental Study of Different Brines in Temperature Swing Solvent Extraction Desalination with Amine Solvents.	
341	Modulating TTA efficiency through control of high energy triplet states 2022, 10, 4923-4928	O
340	Multi-Armed Imide-Based Molecules Promote Interfacial Charge Transfer for Efficient Organic Solar Cells.	
339	A theoretical study on the formation mechanism of carboxylic sulfuric anhydride and its potential role in new particle formation 2022 , 12, 5501-5508	1
338	Computational Investigation of Chemisorption of Thiophosgene on Co@B\$\$_{8}^{-}\$\$. 2022 , 96, 267-272	
337	Ketoprofen-FA Co-crystal: In Vitro and In Vivo Investigation for the Solubility Enhancement of Drug by Design of Expert 2022 , 23, 101	1
336	The role of hydrogen-bond in solubilizing drugs by ionic liquids: A molecular dynamics and density functional theory study.	1
335	Molecular Simulation Study on the Protective Mechanism of Three Kinds of HTPB Propellant Antioxidants. 2022 ,	1
334	A heat-resistant and insensitive energetic material based on the pyrazolo-triazine framework. 2022 , 3, 26-31	1

333	Experimental and theoretical investigation on the thermal isomerization reaction of tristriazolotriazines.	0
332	Antimicrobial activities of two 1-D, 2-D and 3-D mononuclear Mn (II) and dinuclear Bi (III) complexes: X-ray structures, spectroscopic, ESP, HSA and TD/DFT studies.	Ο
331	Study on geometry and chemical activity of twisted cucurbit[13]uril based on density functional theory. 1	
330	The Role of Hydrogen Bonds in Interactions between [PdCl] Dianions in Crystal 2022 , 27,	2
329	Chalcogen Bonding with Diaryl Ditellurides: Evidence from Solid State and Solution Studies 2022,	0
328	Competition between Intra and Intermolecular Pnicogen Bonds. Complexes between Naphthalene Derivatives and Neutral or Anionic Bases 2022 ,	1
327	Molecular insights into the encapsulation of fluorouracil molecule inside the single-walled carbon nanotubes. 2022 , 124, 108900	O
326	New Cu(II) and Zn(II) complexes with diethyl phenyl (N-phenylsulfamoylamino) methyl phosphonate: synthesis, characterisation, DFT/M11 studies, NBO, DOS, QTAIM and RDG analysis. 2022 , 133003	O
325	Effect of polystyrene microplastics on the degradation of sulfamethazine: The role of persistent free radicals 2022 , 155024	О
324	Novel Fe2+ responsive nanofibrous membrane for corrosion detection and adsorption. 2022 , 248, 124817	
323	Separation and recovery of iridium(IV) from simulated secondary resource leachate by extraction - electrodeposition. 2022 , 289, 120765	0
322	Incorporating amino acids functionalized graphene oxide nanosheets into Pebax membranes for CO2 separation. 2022 , 288, 120682	O
321	Equilibrium solubility of amrinone in aqueous co-solvent solutions reconsidered: Quantitative molecular surface, inter/intra-molecular interactions and solvation thermodynamics analysis. 2022 , 355, 118995	2
320	Tuning the mesopore size of lignin-based porous carbon via salt templating for kraft lignin decomposition. 2022 , 181, 114865	
319	Microscopic mechanism and kinetics of NO heterogeneous reduction on char surface: A density functional theory study. 2022 , 250, 123861	0
318	Quantitative surface analysis of paclobutrazol molecule and comprehensive insight into its solubility in aqueous co-solvent solutions. 2022 , 170, 106787	O
317	Dualism of 1,2,4-oxadiazole ring in noncovalent interactions with carboxylic group. 2022 , 1262, 132974	1
316	Multi-armed imide-based molecules promote interfacial charge transfer for efficient organic solar cells. 2022 , 441, 135894	1

315	New silver(I) complex as antibiotic candidate: Synthesis, spectral characterization, DFT, QTAIM and antibacterial investigations and docking properties. 2022 , 1261, 132902	1
314	Insights into the synergistic effect of catalyst acidity and solvent basicity for effective production of pentose from glucose. 2022 , 442, 136224	1
313	Application of Group Theory for Evaluating the Jahn \blacksquare eller Effect and Analyzing the Stability Structure of Boron $\$(\{mathbf\{B\}\}_{\{n,, = ,,(3 - 7)\}}^{\{\{mp,0\}\}})$ \$\$ Clusters. 2021 , 66, 2091-2104	
312	Adsorption of Lewisite Warfare Agent on B12N12 Nano-Cluster: A Computational Investigation. 2021 , 95, 2637-2642	Ο
311	Hapten Synthesis and Monoclonal Antibody Preparation for Simultaneous Detection of Albendazole and Its Metabolites in Animal-Origin Food 2021 , 10,	1
310	Carbazochrome carbon nanotube as drug delivery nanocarrier for anti-bleeding drug: quantum chemical study 2021 , 28, 11	1
309	Interaction between Phosgene and B12N12 Nano-Cluster: A Computational Investigation. 2021 , 95, S323-S3	3 30 0
308	Theoretical Calculation of Cocrystal Components for Explosives: A Similarity Function of Energetic Supramolecules. 2022 , 22, 293-303	1
307	Experimental Methods of Corrosion Inhibition Assessment. 49-60	1
306	Mechanism and Origins of Enantioselectivity of Cobalt-Catalyzed Intermolecular Hydroarylation/Cyclization of 1,6-Enynes with -Pyridylindoles 2022 ,	2
305	Realization of Conceptual Density Functional Theory and Information-Theoretic Approach in Multiwfn Program. 2022 , 631-647	1
304	Mass spectral and theoretical investigations of the N-C bond cleavages in the disulfide-containing peptide TTCPYCKK and its analogues 2022 , e9315	
303	Toxic potential of Poly-hexamethylene biguanide hydrochloride (PHMB): A DFT, AIM and NCI analysis study with solvent effects. 2022 , 1212, 113709	2
302	Quantitative molecular surface analysis of doxofylline and its thermodynamic solubility behavior in aqueous solutions. 2022 , 171, 106792	O
301	2D Benzodithiophene based conjugated polymer/g-C3N4 heterostructures with enhanced photocatalytic activity: Synergistic effect of antibacterial carbazole side chain and main chain copolymerization. 2022 , 312, 121401	1
300	Presentation_1.pdf. 2018 ,	
299	Organometallic-functionalized interfaces for highly efficient inverted perovskite solar cells 2022 , 376, 416-420	81
298	Anion?anion interaction within $Ch(CH)X$ ($Ch = S$, Se , Te ; $X = Cl$, Br , I) dimers stabilized by chalcogen bonds 2022 ,	2

Ultrasensitive and Rapid Colorimetric Detection of Urotropin Boosted by Effective Electrostatic Probing and Non-Covalent Sampling. 1	297	Preference of Adsorption Sites and Electron Transfer Characteristics of Methyl Orange on Hollow Structured Cobalt-Aluminum Layered Double Hydroxides: Experimental and Dft Investigation.	
Boosting the Optical Absorption of Melanin-like Polymers. 2022, 55, 3493-3501 4 Reaction and Transport Co-Intensification Enhanced Continuous Flow Electrocatalytic Aminoxyl-Mediated Oxidation of Sterol Intermediates by 3D Porous Framework Electrode. 2022, 136659 1 292 Mechanisms and Kinetics Studies of Butylated Hydroxytoluene Degradation to Isobutene 2022, 293 Oxel Riuorescent chemosensor sensitively detect copper (II) through the collaboration of quinoline and coumarin groups. 294 Mild Catalytic Mechanism of the Mannich Reaction for Synthesizing Methylacrolein by sec-Amine Short-Chain Alighatic Acid Ionic Liquid Catalysts. 295 Short-Chain Alighatic Acid Ionic Liquid Catalysts. 286 Effects of the Cationic Structure on the Adsorption Performance of Ionic Polymers toward Au(III): 287 an Experimental and DFT Study 2022. 288 Chiral Ferrocenes on polysaccharide-based chiral stationary phases: experimental and electrostatic potential analyses 2022. 1673, 463097 287 Priority Separation of Phenols with Deep Eutectic Solvents from an Acetonitrile-Extractable Portion of a Shale Oil: Experimental and Computational. 288 Ouantitative analysis of molecular surface: systematic application on sodiation mechanism of benzoquinone-based pillared compound as cathode. 289 Dyeing Thermodynamics and Supramolecular Structure of Lac Red on Protein Fibers. 2022, 08, 89-106 280 A Theoretical Study on the Medicinal Properties and Eletronic Structures of Platinum(IV) Anticancer Agents With Cl Substituents. 2022, 12, 281 Theoretical Studies on the Role of Guest in E-CL-20/Guest Crystals. 2022, 27, 3266 282 Quantum Chemical Calculation on the Decomposition Mechanism of Na3AlF6. 2022, 96, 1035-1043 283 Theoretical Studies on the Role of Guest in E-CL-20/Guest Crystals. 2022, 27, 3266 284 Apricating binary cathode interface layer by effective molecular electrostatic potential and interfacial dipole to optimize electron transport and improve organic solar cell. 2022, 137209	296		
Aminoxyl-Mediated Oxidation of Sterol Intermediates by 3D Porous Framework Electrode. 2022, 136659 Mechanisms and Kinetics Studies of Butylated Hydroxytoluene Degradation to Isobutene 2022, Mechanisms and Kinetics Studies of Butylated Hydroxytoluene Degradation to Isobutene 2022, Novel fluorescent chemosensor sensitively detect copper (II) through the collaboration of quinoline and coumarin groups. Mild Catalytic Mechanism of the Mannich Reaction for Synthesizing Methylacrolein by sec-Amine Short-Chain Aliphatic Acid Ionic Liquid Catalysts. Biffects of the Cationic Structure on the Adsorption Performance of Ionic Polymers toward Au(III): an Experimental and DFT Study 2022, Unravelling functions of halogen substituents in the enantioseparation of halogenated planar chiral ferrocenes on polysaccharide-based chiral stationary phases: experimental and electrostatic optential analyses 2022, 1673, 45097 Priority Separation of Phenols with Deep Eutectic Solvents from an Acetonitrile-Extractable Portion of a Shale Oil: Experimental and Computational. 286 Quantitative analysis of molecular surface: systematic application on sodiation mechanism of benzoquinone-based pillared compound as cathode. 287 Dyeing Thermodynamics and Supramolecular Structure of Lac Red on Protein Fibers. 2022, 08, 89-106 288 ATheoretical Study on the Medicinal Properties and Eletronic Structures of Platinum(IV) Anticancer Agents With CI Substituents. 2022, 12, 2 289 Theoretical Studies on the Role of Guest in B-CL-20/Guest Crystals. 2022, 27, 3266 O Theoretical Studies on the Role of Guest in B-CL-20/Guest Crystals. 2022, 27, 3266 O Theoretical Studies on the Role of Guest in B-CL-20/Guest Crystals. 2022, 27, 3266 O Theoretical Studies on the Role of Guest in B-CL-20/Guest Crystals. 2022, 27, 3266 O Theoretical Studies on the Role of Guest in B-CL-20/Guest Crystals. 2022, 27, 3266 O Theoretical Studies on the Role of Guest in B-CL-20/Guest Crystals. 2022, 27, 3266	295	Iodous acid-a more efficient nucleation precursor than iodic acid.	1
Aminoxyl-Mediated Oxidation of Sterol Intermediates by 3D Porous Framework Electrode. 2022, 136659 Mechanisms and Kinetics Studies of Butylated Hydroxytoluene Degradation to Isobutene 2022, Movel Fluorescent chemosensor sensitively detect copper (II) through the collaboration of quinoline and coumarin groups. Mild Catalytic Mechanism of the Mannich Reaction for Synthesizing Methylacrolein by sec-Amine Short-Chain Aliphatic Acid Ionic Liquid Catalysts. Effects of the Cationic Structure on the Adsorption Performance of Ionic Polymers toward Au(III): an Experimental and DFT Study 2022, Unravelling functions of halogen substituents in the enantioseparation of halogenated planar chiral ferrocenes on polysaccharide-based chiral stationary phases: experimental and electrostatic potential analyses 2022, 1673, 463097 Priority Separation of Phenols with Deep Eutectic Solvents from an Acetonitrile-Extractable Portion of a Shale Oil: Experimental and Computational. Quantitative analysis of molecular surface: systematic application on sodiation mechanism of benzoquinone-based pillared compound as cathode. Dyeing Thermodynamics and Supramolecular Structure of Lac Red on Protein Fibers. 2022, 08, 89-106 A Theoretical Study on the Medicinal Properties and Eletronic Structures of Platinum(IV) Anticancer Agents With Cl Substituents. 2022, 12, Theoretical Studies on the Role of Guest in R-CL-20/Guest Crystals. 2022, 27, 3266 Quantum Chemical Calculation on the Decomposition Mechanism of Na3AlF6. 2022, 96, 1035-1043 Theoretical Studies on the Role of Guest in R-CL-20/Guest Crystals. 2022, 27, 3266 Liquid-Liquid Extraction and Mechanism Exploration for Separation of Mixture	294	Boosting the Optical Absorption of Melanin-like Polymers. 2022 , 55, 3493-3501	4
Novel fluorescent chemosensor sensitively detect copper (II) through the collaboration of quinoline and coumarin groups. 290 Mild Catalytic Mechanism of the Mannich Reaction for Synthesizing Methylacrolein by sec-Amine Short-Chain Aliphatic Acid Ionic Liquid Catalysts. 289 Effects of the Cationic Structure on the Adsorption Performance of Ionic Polymers toward Au(III): an Experimental and DFT Study 2022, 280 Unravelling functions of halogen substituents in the enantioseparation of halogenated planar chiral ferrocenes on polysaccharide-based chiral stationary phases: experimental and electrostatic opotential analyses 2022, 1673, 463097 287 Priority Separation of Phenols with Deep Eutectic Solvents from an Acetonitrile-Extractable Portion of a Shale Oil: Experimental and Computational. 286 Quantitative analysis of molecular surface: systematic application on sodiation mechanism of benzoquinone-based pillared compound as cathode. 287 Dyeing Thermodynamics and Supramolecular Structure of Lac Red on Protein Fibers. 2022, 08, 89-106 288 A Theoretical Study on the Medicinal Properties and Eletronic Structures of Platinum(IV) Anticancer Agents With Cl Substituents. 2022, 12, 289 Theoretical Studies on the Role of Guest in B-CL-20/Guest Crystals. 2022, 27, 3266 280 Quantum Chemical Calculation on the Decomposition Mechanism of Na3AlF6. 2022, 96, 1035-1043 281 Fabricating binary cathode interface layer by effective molecular electrostatic potential and interfacial dipole to optimize electron transport and improve organic solar cell. 2022, 137209 10 10 10 10 10 10 10 10 10 10 10 10 10 1	293		1
quinoline and coumarin groups. Mild Catalytic Mechanism of the Mannich Reaction for Synthesizing Methylacrolein by sec-Amine Short-Chain Aliphatic Acid Ionic Liquid Catalysts. Effects of the Cationic Structure on the Adsorption Performance of Ionic Polymers toward Au(III): an Experimental and DFT Study 2022, Unravelling functions of halogen substituents in the enantioseparation of halogenated planar chiral Ferrocenes on polysaccharide-based chiral stationary phases: experimental and electrostatic opotential analyses 2022, 1673, 463097 Priority Separation of Phenols with Deep Eutectic Solvents from an Acetonitrile-Extractable Portion of a Shale Oil: Experimental and Computational. 286 Quantitative analysis of molecular surface: systematic application on sodiation mechanism of benzoquinone-based pillared compound as cathode. 285 Dyeing Thermodynamics and Supramolecular Structure of Lac Red on Protein Fibers. 2022, 08, 89-106 284 A Theoretical Study on the Medicinal Properties and Eletronic Structures of Platinum(IV) Anticancer Agents With Cl Substituents. 2022, 12, 283 Theoretical Studies on the Role of Guest in B-CL-20/Guest Crystals. 2022, 27, 3266 O 284 Quantum Chemical Calculation on the Decomposition Mechanism of Na3AlF6. 2022, 96, 1035-1043 O 285 Effects of the Cationic Structure of Lac Red on Protein Fibers. 2022, 137209 1 1 286 Indicating binary cathode interface layer by effective molecular electrostatic potential and interfacial dipole to optimize electron transport and improve organic solar cell. 2022, 137209 1 287 Eliquid-Liquid Extraction and Mechanism Exploration for Separation of Mixture	292	Mechanisms and Kinetics Studies of Butylated Hydroxytoluene Degradation to Isobutene 2022,	O
Short-Chain Aliphatic Acid Ionic Liquid Catalysts. Effects of the Cationic Structure on the Adsorption Performance of Ionic Polymers toward Au(III): an Experimental and DFT Study 2022, Unravelling functions of halogen substituents in the enantioseparation of halogenated planar chiral ferrocenes on polysaccharide-based chiral stationary phases: experimental and electrostatic potential analyses 2022, 1673, 463097 Priority Separation of Phenols with Deep Eutectic Solvents from an Acetonitrile-Extractable Portion of a Shale Oil: Experimental and Computational. Quantitative analysis of molecular surface: systematic application on sodiation mechanism of benzoquinone-based pillared compound as cathode. Dyeing Thermodynamics and Supramolecular Structure of Lac Red on Protein Fibers. 2022, 08, 89-106 A Theoretical Study on the Medicinal Properties and Eletronic Structures of Platinum(IV) Anticancer Agents With Cl Substituents. 2022, 12, Theoretical Studies on the Role of Guest in B-CL-20/Guest Crystals. 2022, 27, 3266 Quantum Chemical Calculation on the Decomposition Mechanism of Na3AlF6. 2022, 96, 1035-1043 o Fabricating binary cathode interface layer by effective molecular electrostatic potential and interfacial dipole to optimize electron transport and improve organic solar cell. 2022, 137209 Liquid-Liquid Extraction and Mechanism Exploration for Separation of Mixture	291		
an Experimental and DFT Study 2022, Unravelling functions of halogen substituents in the enantioseparation of halogenated planar chiral ferrocenes on polysaccharide-based chiral stationary phases: experimental and electrostatic potential analyses 2022, 1673, 463097 Priority Separation of Phenols with Deep Eutectic Solvents from an Acetonitrile-Extractable Portion of a Shale Oil: Experimental and Computational. 286 Quantitative analysis of molecular surface: systematic application on sodiation mechanism of benzoquinone-based pillared compound as cathode. Dyeing Thermodynamics and Supramolecular Structure of Lac Red on Protein Fibers. 2022, 08, 89-106 286 A Theoretical Study on the Medicinal Properties and Eletronic Structures of Platinum(IV) Anticancer Agents With Cl Substituents. 2022, 12, 287 Theoretical Studies on the Role of Guest in 8-CL-20/Guest Crystals. 2022, 27, 3266 Quantum Chemical Calculation on the Decomposition Mechanism of Na3AlF6. 2022, 96, 1035-1043 December 2022, 137209 1 Eabricating binary cathode interface layer by effective molecular electrostatic potential and interfacial dipole to optimize electron transport and improve organic solar cell. 2022, 137209 Liquid-Liquid Extraction and Mechanism Exploration for Separation of Mixture	2 90		O
chiral ferrocenes on polysaccharide-based chiral stationary phases: experimental and electrostatic potential analyses 2022, 1673, 463097 Priority Separation of Phenols with Deep Eutectic Solvents from an Acetonitrile-Extractable Portion of a Shale Oil: Experimental and Computational. 286 Quantitative analysis of molecular surface: systematic application on sodiation mechanism of benzoquinone-based pillared compound as cathode. 285 Dyeing Thermodynamics and Supramolecular Structure of Lac Red on Protein Fibers. 2022, 08, 89-106 286 A Theoretical Study on the Medicinal Properties and Eletronic Structures of Platinum(IV) Anticancer Agents With CI Substituents. 2022, 12, 287 Theoretical Studies on the Role of Guest in E-CL-20/Guest Crystals. 2022, 27, 3266 288 Quantum Chemical Calculation on the Decomposition Mechanism of Na3AlF6. 2022, 96, 1035-1043 289 Fabricating binary cathode interface layer by effective molecular electrostatic potential and interfacial dipole to optimize electron transport and improve organic solar cell. 2022, 137209	289		1
Portion of a Shale Oil: Experimental and Computational. Quantitative analysis of molecular surface: systematic application on sodiation mechanism of benzoquinone-based pillared compound as cathode. Dyeing Thermodynamics and Supramolecular Structure of Lac Red on Protein Fibers. 2022, 08, 89-106 A Theoretical Study on the Medicinal Properties and Eletronic Structures of Platinum(IV) Anticancer Agents With Cl Substituents. 2022, 12, Theoretical Studies on the Role of Guest in #-CL-20/Guest Crystals. 2022, 27, 3266 Quantum Chemical Calculation on the Decomposition Mechanism of Na3AlF6. 2022, 96, 1035-1043 Pabricating binary cathode interface layer by effective molecular electrostatic potential and interfacial dipole to optimize electron transport and improve organic solar cell. 2022, 137209 Liquid-Liquid Extraction and Mechanism Exploration for Separation of Mixture	288	chiral ferrocenes on polysaccharide-based chiral stationary phases: experimental and electrostatic	O
benzoquinone-based pillared compound as cathode. Dyeing Thermodynamics and Supramolecular Structure of Lac Red on Protein Fibers. 2022, 08, 89-106 A Theoretical Study on the Medicinal Properties and Eletronic Structures of Platinum(IV) Anticancer Agents With Cl Substituents. 2022, 12, Theoretical Studies on the Role of Guest in B-CL-20/Guest Crystals. 2022, 27, 3266 Quantum Chemical Calculation on the Decomposition Mechanism of Na3AlF6. 2022, 96, 1035-1043 Fabricating binary cathode interface layer by effective molecular electrostatic potential and interfacial dipole to optimize electron transport and improve organic solar cell. 2022, 137209 Liquid-Liquid Extraction and Mechanism Exploration for Separation of Mixture	287		
A Theoretical Study on the Medicinal Properties and Eletronic Structures of Platinum(IV) Anticancer Agents With Cl Substituents. 2022, 12, Theoretical Studies on the Role of Guest in 8-CL-20/Guest Crystals. 2022, 27, 3266 Quantum Chemical Calculation on the Decomposition Mechanism of Na3AlF6. 2022, 96, 1035-1043 Fabricating binary cathode interface layer by effective molecular electrostatic potential and interfacial dipole to optimize electron transport and improve organic solar cell. 2022, 137209 Liquid-Liquid Extraction and Mechanism Exploration for Separation of Mixture	286	Quantitative analysis of molecular surface: systematic application on sodiation mechanism of benzoquinone-based pillared compound as cathode.	O
Agents With Cl Substituents. 2022, 12, Theoretical Studies on the Role of Guest in \(\text{H-CL-20/Guest Crystals.}\) 2022, 27, 3266 Quantum Chemical Calculation on the Decomposition Mechanism of Na3AlF6. 2022, 96, 1035-1043 Fabricating binary cathode interface layer by effective molecular electrostatic potential and interfacial dipole to optimize electron transport and improve organic solar cell. 2022, 137209 Liquid-Liquid Extraction and Mechanism Exploration for Separation of Mixture	285	Dyeing Thermodynamics and Supramolecular Structure of Lac Red on Protein Fibers. 2022, 08, 89-106	
Quantum Chemical Calculation on the Decomposition Mechanism of Na3AlF6. 2022, 96, 1035-1043 Fabricating binary cathode interface layer by effective molecular electrostatic potential and interfacial dipole to optimize electron transport and improve organic solar cell. 2022, 137209 Liquid-Liquid Extraction and Mechanism Exploration for Separation of Mixture	284		
Fabricating binary cathode interface layer by effective molecular electrostatic potential and interfacial dipole to optimize electron transport and improve organic solar cell. 2022 , 137209 Liquid-Liquid Extraction and Mechanism Exploration for Separation of Mixture	283	Theoretical Studies on the Role of Guest in ∃-CL-20/Guest Crystals. 2022 , 27, 3266	O
interfacial dipole to optimize electron transport and improve organic solar cell. 2022 , 137209 Liquid-Liquid Extraction and Mechanism Exploration for Separation of Mixture	282	Quantum Chemical Calculation on the Decomposition Mechanism of Na3AlF6. 2022 , 96, 1035-1043	O
	281		1
	280		0

279	Acetamiprid in several binary aqueous solutions: Solubility, intermolecular interactions and solvation behavior. 2022 , 172, 106828	0
278	Computational and experimental study of different brines in temperature swing solvent extraction desalination with amine solvents. 2022 , 537, 115863	1
277	Understanding the interaction of N-doped graphene and sulfur compounds in a lithium-sulfur battery \Box density functional theory investigation.	0
276	Diversity-Oriented Synthesis of Functional Polymers with Multisubstituted Small Heterocycles by Facile Stereoselective Multicomponent Polymerizations.	1
275	The mechanisms and molecular properties about isomerization of resin acids, synthesis of acrylopimaric acid based on DFT Calculation.	
274	Desensitizing high energy materials HMX and CL-20 by the smallest all carbon compound cyclo[18]carbon: a DFT study.	О
273	Study of Butylated Hydroxytoluene Inhibiting the Coal Oxidation at Low Temperature: Combining Experiments and Quantum Chemical Calculations.	0
272	Intercalating negatively charged pillars into graphene oxide sheets to enhance sulfonamide pharmaceutical removal from water.	O
271	Molecules with a TEMPO-based head group as high-performance organic friction modifiers.	0
270	Composition-selective full inclusion hostguest interaction of azobenzene-containing photoresponsive nanoring with fullerene C 60 .	1
269	Alkali Resistance Mechanism of Cyano-containing Heterocyclic Disperse Dyes. 2022, 133438	
268	Photo- and Electroluminescent Neutral Iridium(III) Complexes Bearing Imidoylamidinate Ligands.	1
267	Ultrasensitive and rapid colorimetric detection of urotropin boosted by effective electrostatic probing and non-covalent sampling. 2022 , 436, 129263	0
266	Magnetic powdery acrylic polymer with ultrahigh adsorption capacity for atenolol removal: Preparation, characterization, and microscopic adsorption mechanism. 2022 , 446, 137175	1
265	Synthesis and investigations of reactive properties, photophysical properties and biological activities of a pyrazole-triazole hybrid molecule. 2022 , 1265, 133363	3
264	Competing on the same stage: Ru-based catalysts modified by basic ligands and organic chlorine salts for acetylene hydrochlorination.	O
263	<i>N</i> -Halamine-Based Nanosilver Surface Engineering for Efficient Antibiotic-Resistant Bacteria Eradication.	
262	Effect of Alkyl Chain Length on High-Temperature Corrosion Inhibition Behavior and Mechanism of Imidazole Ionic Liquids: An Experimental, Density Functional Theory and Molecular Dynamics Simulation Study.	

261	PTSA-catalyzed selective synthesis and antibacterial evaluation of 1,2-disubstituted benzimidazoles.	О
260	Theoretical investigation on the interactions of microplastics with a SARS-CoV-2 RNA fragment and their potential impacts on viral transport and exposure. 2022 , 156812	O
259	Experimental and theoretical investigations of lithium isotopes separation using 10-hydroxybenzoquinoline.	0
258	Virtual Experiments on Real Asphaltenes: Predicting Properties Using Quantum Chemical Simulations of Structures from Non-contact Atomic Force Microscopy.	1
257	Domination of H-Bond Interactions in the Solvent-Triggering Gelation Process.	1
256	Spectroscopic studies, TD/DFT calculations, electrochemical, antibacterial, and Hirshfeld surface analysis of Ni(II) and Co(III) complexes based on 3-ethoxy salicylaldehyde. 2022 , 133554	O
255	Fine-tuning the Ibridge of organic dye molecules with triarylamino as an electron donor by using electron-rich/deficient groups for more efficient dye-sensitized solar cells.	
254	Quantitative surface and Hirshfeld surface analysis of nicorandil molecule and further insight into its solubility in several aqueous protic and aprotic cosolvent solutions. 2022 , 119697	O
253	Ag Atom Anchored on Defective Hexagonal Boron Nitride Nanosheets As Single Atom Adsorbents for Enhanced Adsorptive Desulfurization via S-Ag Bonds. 2022 , 12, 2046	2
252	Comparative study on organic solvents and green solvents in separation of aromatic hydrocarbons/low-carbon alcohols azeotrope by structureEctivity relationship. 2022 , 297, 121498	O
251	Weak antiferromagnetic interaction in Cu(ii) complex with semi-coordination exchange pathway. 2022 , 223, 115962	1
250	Inter-/intra-molecular interactions, preferential solvation, and dissolution and transfer property for tirofiban in aqueous co-solvent mixtures. 2022 , 361, 119665	1
249	Synergistic enhancement of piezocatalysis and electrochemical oxidation for the degradation of ciprofloxacin by PbO2 intercalation material. 2022 , 297, 121528	О
248	Mechanism of the Fe(iii)-catalyzed synthesis of hexahydropyrimidine with ∃-phenylstyrene: a DFT study. 2022 , 12, 20523-20529	
247	The sensitive detection and mechanism of Fe-3,5-dimethyl pyrazole fluorescent sensor to diethylenetriamine pentamethylene phosphonic acid: experimental study and quantum chemical calculation. 2022 , 121623	
246	Molecular doped, color-tunable, high-mobility, emissive, organic semiconductors for light-emitting transistors. 2022 , 8,	4
245	Substitution Effects on the Reactivity and Thermostability of Five-Membered Ring Fluorides.	
244	Combined Experimental and Computational Study on the Transformation of a Novel 1,3,4-Oxadiazole Thioether Nematicide in Aqueous Solutions.	O

243	Hollow Covalent Organic Framework with Bhell-Confined Environment for the Effective Removal of Anionic Per- and Polyfluoroalkyl Substances. 2203171	O
242	Experimental and theoretical insights into two fluorine-containing imidazoline Schiff base inhibitors for carbon steels in hydrochloric acid solution. 2022 , 133737	1
241	Quantifying the anion effect of gas solubility within ionic liquids using the solvation affinity index. 2022 , 260, 117851	О
2 40	Deep removal of chlorobenzene based volatile organic compounds from exhaust gas with ionic liquids. 2022 , 298, 121610	1
239	Efficient removal of heavy metal ions by diethylenetriaminepenta (methylene phosphonic) acid-doped hydroxyapatite. 2022 , 157557	O
238	Internal electric field-mediated sulfur vacancy-modified-In2S3/TiO2 thin-film heterojunctions as a photocatalyst for peroxymonosulfate activation: Density functional theory calculations, levofloxacin hydrochloride degradation pathways and toxicity of intermediates. 2022 , 138271	1
237	Impact of the Dicarboxylic Acid Chain Length on Intermolecular Interactions with Lidocaine.	
236	DFT Investigation of Polyethylene-co-vinyl Acetate: Kinetics of Initiation and Propagation, Copolymer Composition, and Unit Sequence Distribution.	
235	Achieving the low interfacial tension by balancing crystallization and film-forming ability of the cathode interlayer for organic solar cells. 2022 , 627, 880-890	0
234	The Extraction of Aromatics Using Nmp: Liquid-Liquid Equilibrium Determination and Mechanistic Exploration.	
233	Two mono- and dinuclear Bi(III) complexes combined with crystallographic, spectroscopic, and antibacterial activities, MEP/HSA, and TD/DFT calculations.	O
232	Sensitive fluorescent detection and micromechanism of Mn-doped CuS probe for oxytetracycline hydrochloride. 2022 , 121768	O
231	Breaking through the Separation Barrier of Zr(IV) and Hf(IV): Magical Effect of the Bisamide Ligand.	
230	A small addition of reduced graphene oxide to protect fluorosilicone rubber from thermal oxidative degradation.	
229	Cyclized oligomer of tetracyanoquinodimethane-tetrathiafulvalene (TCNQ-TTF): a versatile macrocyclic molecule by DFT calculations.	
228	Experimental and Quantum Chemical Study on the Inhibition Characteristics of Glutathione to Coal Oxidation at Low Temperature.	
227	Improving the solubility, hygroscopicity and permeability of enrofloxacin by forming 1:2 pharmaceutical salt cocrystal with neutral and anionic co-existing p-nitrobenzoic acid. 2022 , 103732	1
226	Developing new derivatives of 3-X-4-hydroxy-2(1 H)-quinolone as quinoline-based chemosensors for detecting fluoride: Theoretical study on nucleophilicity and hydrogen-bonding via various analyses.	

225	The facile detection and micromechanism of ATMP and DTPMP by fluorescence sensor based on nitrogen-doped carbon nanomaterials. 2022 , 110659	
224	Stability, atomic charges, bond-order analysis, and the directionality of lone-electron pairs on nitriles and isocyanides.	Ο
223	Comparative study of the hydrogen bonding properties between allyl-functionalized/non-functionalized ionic liquids and DMSO. 2022 , 122, 103412	0
222	An investigation on chain transfer to monomers and initiators, termination of radicals in EVA copolymerization process based on DFT and microkinetic simulation. 2022 , 256, 125181	
221	Acylating blueberry anthocyanins with fatty acids: Improvement of their lipid solubility and antioxidant activities. 2022 , 15, 100420	0
220	Density Functional Study of the adsorption behavior of 6-mercaptopurine on Primary, Si, Al and Ti doped C60 fullerenes. 2022 , 804, 139910	Ο
219	Selective extraction of Nd(III) by novel carboxylic acid based ionic liquids without diluent from waste NdFeB magnets. 2022 , 364, 119919	1
218	Electronic structure calculations of the fundamental interactions in solvent extraction desalination. 2022 , 364, 119986	Ο
217	3-Nitrophthalonitrile solubility and solvation thermodynamics in aqueous solutions. 2022 , 174, 106873	
216	A silane-based coupling strategy for enhancing the mechanical properties of proanthocyanidin nanocoatings on Ti dental implants. 2022 , 602, 154400	Ο
215	Synergistic co-reaction of Zn2+ and H+ with carbonyl groups towards stable aqueous zinc@rganic batteries. 2022 , 52, 386-394	1
214	Revealing the non-covalent interactions between oxygen-containing demulsifiers and interfacially active asphaltenes: A multi-level computational simulation. 2022 , 329, 125375	Ο
213	N-doped carbon intercalated Fe-doped MoS2 nanosheets with widened interlayer spacing: An efficient peroxymonosulfate activator for high-salinity organic wastewater treatment. 2022 , 628, 318-330	0
212	An iron chlorophyll derivative for enhanced degradation of bisphenol A: New insight into the generation mechanism of high-valent iron oxo species. 2023 , 451, 138688	
211	Hydrogen Bond Effects: A Strategy for Improving Controllability in Organocatalytic Photoinduced Controlled Radical Polymerization Targeting High Molecular Weight. 11606-11614	0
210	Effect of caffeic acid esters on antioxidant activity and oxidative stability of sunflower oil: Molecular simulation and experiments. 2022 , 160, 111760	O
209	A separation strategy of Au(III), Pd(II) and Pt(IV) based on hydrophobic deep eutectic solvent from hydrochloric acid media. 2022 , 365, 120200	2
208	Comparative study on the deep eutectic solvents formed by choline chloride and cresol isomers from theoretical and experimental perspectives. 2022 , 367, 120420	O

207	Radical-induced pyrolysis mechanism in CalD and CalDal bond cleavage. 2022, 238, 107494	O
206	Transdermal release behaviors of bioactive deep eutectic solvents as natural skin care and mechanism. 2022 , 367, 120412	1
205	Comprehending of florfenicol (form A) dissolution behavior in aqueous low alcohol blends: Solubility, solvation thermodynamics as well as inter-molecular interactions. 2023 , 176, 106925	O
204	Adsorption Sites and Electron Transfer Characteristics of Methyl Orange on Three-Dimensional Hierarchical Flower-Like Nanostructures of Co-Al-Layered Double Hydroxides: Experimental and Dft Investigation.	O
203	Hydroboration of carbon dioxide with pinacolborane catalyzed by various aluminum hydrides: a comparative mechanistic study.	O
202	Flexibility is the key to tuning the transport properties of fluorinated imide-based ionic liquids. 2022 , 13, 9176-9190	O
201	Comprehending radicals, diradicals and their bondings in aggregates of imide-fused polycyclic aromatic hydrocarbons. 2022 , 13, 9985-9992	O
200	In-Situ Growth of 2d Magnesium Hydroxide on Zirconium-Based Metal Organic Frameworks for Phosphate Removal: An Experimental and Theoretical Exploration of Adsorption Behavior.	O
199	Interaction-determined extraction capacity between rare earth ions and extractants: taking lanthanum and lutetium as models through theoretical calculations.	1
198	Molecular reaction and dynamic mechanism of iodate reduction to molecular iodine by nitrogen(iii) in aqueous solution. 2022 , 24, 22889-22897	O
197	Molecular tuning non-fullerene electron acceptor in organic photovoltaics: a theoretical study.	O
196	A three dimensional graphdiyne-like porous triptycene network for gas adsorption and separation. 2022 , 12, 28299-28305	O
195	Two-dimensional covalent organic frameworks with p- and bipolar-type redox-active centers for organic high-performance Li-ion battery cathodes. 2022 , 10, 16595-16601	1
194	Molecular dynamics simulation study of adsorption of anionicflonionic surfactants at oil/water interfaces. 2022 , 12, 27330-27343	O
193	A comprehensive study on the photophysical and non-linear optical properties of thienyl-chalcone derivatives. 2022 , 24, 21927-21953	O
192	Nitazoxanide in aqueous co-solvent solutions of isopropanol/DMF/NMP: Solubility, solvation thermodynamics and intermolecular interactions. 2023 , 176, 106928	1
191	Developing a QSPR Model of Organic Carbon Normalized Sorption Coefficients of Perfluorinated and Polyfluoroalkyl Substances. 2022 , 27, 5610	0
190	A Competitive Solvation of Ternary Eutectic Electrolytes Tailoring the Electrode/Electrolyte Interphase for Lithium Metal Batteries. 2022 , 16, 14558-14568	1

189	Anion Photoelectron Spectroscopy and Quantum Chemical Calculations of Bimetallic Oxide Clusters YCu2On[10 (n = 28). 2022 , 126, 6067-6079	O
188	From NH Nitration to Controllable Aromatic Mononitration and Dinitration-The Discovery of a Versatile and Powerful N-Nitropyrazole Nitrating Reagent. 2022 , 2, 2152-2161	O
187	Enhancement of SO2 sensing performance of micro-ribbon graphene sensors using nitrogen doping and light exposure. 2022 , 155059	1
186	The ionic salts with super oxidizing ions O2+ and N5+: Potential candidates for high-energy oxidants. 10,	O
185	Improving the performance of DSSCs by modulating the electron donor and electron acceptor of dye molecules with the DTPBT group as Ebridge.	0
184	Enantioseparation of planar chiral ferrocenes on cellulose-based chiral stationary phases: Benzoate versus carbamate pendant groups.	O
183	Microscopic reaction mechanism for CO2 gasification of cellulose based on reactive force field molecular dynamics simulations. 2022 ,	O
182	Ionization of Decamethylmanganocene: Insights from the DFT-Assisted Laser Spectroscopy. 2022 , 27, 6226	O
181	A novel design method for TPMS lattice structures with complex contour based on moving elements method.	O
180	Deep Trap Origins, Characteristics, and Related Mechanisms in Chemically Grafted Polypropylene with Enhanced Direct Current Volume Resistivity. 2022 , 126, 16280-16288	O
179	s-Holes in Iodonium Ylides: Halogen-Bond Activation of Carboxylic Acids, Phenols and Thiophenols May Enable Their X⊞ Insertion Reactions.	1
178	Semi-Empirical Calculation of Bodipy Aggregate Spectroscopic Properties through Direct Sampling of Configurational Ensembles. 2022 , 23, 10955	O
177	Mixed-Isocyanide Complexes of Technetium under Steric and Electronic Control.	2
176	Molecular Dynamics Research of Spatial Orientation and Kinetic Energy of Active Site Collision of Carnosine under Weak Microwave Irradiation. 2022 , 126, 7686-7700	O
175	Methionine-Derived Organogels as Lubricant Additives Enhance the Continuity of the Oil Film through Dynamic Self-Healing Assembly. 2022 , 38, 11492-11501	O
174	Effect of Ligand Structures on Ligand-Protected Gold Clusters: [Au[þ-/m-/o-MBT)]18 Clusters.	O
173	In-situ growth of 2D magnesium hydroxide on zirconium-based metal organic frameworks for phosphate removal: An experimental and theoretical exploration of adsorption behavior. 2022 , 122289	O
172	Liquid[liquid Equilibrium Experiment and Mechanism Study on the System of Dimethyl Carbonate + n-Propanol + Ionic Liquids.	O

171	StructureBroperties relationships of deep eutectic solvents formed between choline chloride and carboxylic acids: Experimental and computational study. 2022 , 134283	O
170	Molecular-based asphalt oxidation reaction mechanism and aging resistance optimization strategies based on quantum chemistry. 2022 , 111225	1
169	Insight into the weak interaction between organic primary amine and propionic acid or phenol solvents in solvent extraction. 2022 , 120524	O
168	Experimental and quantum chemical study on the inhibition characteristics of triphenyl phosphite to lignite oxidation at low temperature. 2022 , 717, 179358	O
167	Adsorption sites and electron transfer characteristics of methyl orange on three-dimensional hierarchical flower-like nanostructures of Co-Al-layered double hydroxides: Experimental and DFT investigation. 2022 , 303, 122282	O
166	Modelling the octanol-air partition coefficient of aromatic pollutants based on the solvation free energy and the dimer effect. 2022 , 309, 136608	O
165	I?N halogen bonding in 1 : 1 co-crystals formed between 1,4-diiodotetrafluorobenzene and the isomeric n-pyridinealdazines (n = 2, 3 and 4): assessment of supramolecular association and influence upon solid-state photoluminescence properties.	1
164	Extraction of Au(iii) from hydrochloric acid media using a novel amide-based ionic liquid. 2022 , 46, 19824-1983	33 <u>í</u>
163	A broadly applicable quantitative relative reactivity model for nucleophilic aromatic substitution (SNAr) using simple descriptors.	О
162	Origin of Humidity Influencing the Excited State Electronic Properties of Silicon Quantum Dots based Light-emitting Diodes.	O
161	Nanopockets with a Thermoresponsive Nitrate Ionic Liquid for Highly Efficient Uranium Extraction at High Acidity. 2022 , 5, 14893-14901	0
160	Theoretical insights into the roles of intermolecular interactions in BTATz-based solvate cocrystals.	О
159	Preparation of polyether amine-bridged lignosulfonate for utilization as a nano dye dispersant. 2022 ,	O
158	Synthesis, spectroscopic studies, and single-crystal structures of two 3-D supramolecular zinc(II) and nickel(II) complexes containing thiazole ring: Antimicrobial assays, time-dependent density functional theory calculations, and Hirshfeld surface analysis.	O
157	Constructing Nonaqueous Rechargeable Zinc-Ion Batteries with Zinc Trifluoroacetate. 2022 , 5, 12437-12447	О
156	CHEMISORPTION OF C2H2 ON C20 BOWL: A COMPUTATIONAL INVESTIGATION. 2022 , 63, 1600-1609	О
155	Polychlorinated Biphenyls Interactions with Water Characterization Based on the Analysis of Non-Covalent Interactions and Energy Partitioning. 2022 , 14, 12529	O
154	Thionation toward High-Contrast ACQ-DIE Probes by Reprogramming the Aqueous Segregation Behavior: Enlightenment from a Sulfur-Substituted G-Quadruplex Ligand.	1

153	Chiral ionic liquid-multi walled carbon nanotubes composite membrane applied to the separation of amino acid enantiomers. 2022 , 463630	1
152	Pharmaceutical Salts of Piroxicam and Meloxicam with Organic Counterions. 2022 , 22, 6504-6520	1
151	Complexes of carbon dioxide with methanol and its monohalogen-substituted: beyond the tetrel bond. 2022 , 140158	0
150	Quantum Chemical Investigations on the Hydrogen-Bonded Interactions of Bioactive Molecule N2-(4-Methoxysalicylidene) Arginine Hemihydrate. 1-22	O
149	Theoretical Investigation on Interactions between N-methylpyrrolidone-FeCl3 and Components in Model Oil: The Role of S-Fe Coordination in Thiophene Removal. 2022 , 120719	O
148	Structural microheterogeneity and hydrogen bonding properties in the mixtures of two ionic liquids with a common imidazolium cation. 2022 , 368, 120594	0
147	Application for the porous structure of cellulose separators: Ionic conduction path in lithium-ion battery. 2022 , 926, 116937	O
146	Effect of hydroxyl functional groups on SO2 adsorption by activated carbon. 2022 , 10, 108727	O
145	Enhancement of polysiloxane/epoxy resin compatibility through an electrostatic and van der Waals potential design strategy. 2023 , 117, 107820	0
144	Solubility, solvent effect, preferential solvation and DFT computations of 5-nitrosalicylic acid in several aqueous blends. 2023 , 177, 106936	1
143	Combined experimental, computational studies (synthesis, crystal structural, DFT calculations, spectral analysis) and biological evaluation of the new homonuclear complex Di-Ū-benzoato-bis [benzoatodipyridine-cobalt (II)]. 2023 , 1273, 134331	0
142	Experimental and quantum chemical calculations investigations of morpholine-based ionic liquids as extractants for efficient extraction of nitrogen heterocyclic neutral compounds. 2023 , 333, 126446	Ο
141	Study on catalytic activity of polypeptides toward hydrolysis of glucoside compounds gastrodin, polydatin and esculin.	0
140	Antioxidant mechanisms and products of four 4屆,7-trihydroxyflavonoids with different structural types.	O
139	Balance of sulfur doping content and conductivity of hard carbon anode for high-performance K-ion storage. 2023 , 54, 668-679	1
138	Understanding adsorption mechanisms of mercury over unburned carbon. 2023 , 333, 126399	0
137	Unusual oxygenBxygen dichalcogen bond in an oxo-centered trinclear iron coordination cluster. 2023 , 1274, 134318	О
136	Synthesis of coplanar quaternary ammonium salts with excellent electrochemical properties based on an anthraquinone skeleton and their application in copper plating. 2022 , 141541	O

135	Theoretical Exploration of Peculiar Sandwich-Type Clusters Formed by the Coordination of E92[[E = Si, Ge, Sn) Zintl Clusters: Structural Properties, Active Sites, and Hydrogen Storage.	O
134	Five Cocrystal Forms of Antitumor Drug Temozolomide with p-Hydroxybenzoic Acid: Structure, Computational Analysis, Characterizations, Stability, and Transformation.	O
133	Computational assessment of herbal medicine-derived compounds as potential inhibitors of SARS-CoV-2 main protease. 1-12	O
132	Mechanism Analysis of Ethanol Production from Cellulosic Insulating Paper Based on Reaction Molecular Dynamics. 2022 , 14, 4918	O
131	Chalcogen Bond as a Factor Stabilizing Ligand Conformation in the Binding Pocket of Carbonic Anhydrase IX Receptor Mimic. 2022 , 23, 13701	2
130	Atmospheric chemistry of CF3C CH: Kinetics, products, mechanism of gas-phase reaction with OH radicals, and atmospheric implications-an effort for novel Elass of refrigerant. 2022 , 119467	O
129	Insertion Reaction of Me3SiN3 with Bis(germylene).	O
128	What is the role of phytochemical compounds as capping agents for the inhibition of aggregation in the green synthesis of metal oxide nanoparticles? A DFT molecular level response. 2022 , 110243	O
127	High proton conductivity modulated by active protons in 1D ultra-stable metal-organic coordination polymers:a new insight into coordination interaction/ability of metal ion.	O
126	Intrinsic influence of selenium substitution in thiophene and benzo-2,1,3-thiadiazole on the electronic structure, excited states and photovoltaic performances evaluated using theoretical calculations.	O
125	Sodium complexes as precise tools for cutting polymer chains. Exploration of PLA degradation by unique cooperation of sodium centers.	O
124	Screening, packing systematics, Hansen solubility parameters and desolvation of resmetirom (MGL-3196) solvates. 2023 , 369, 120857	O
123	Design and theoretical studies of FOX-7-like novel energetic compounds.	O
122	Theoretical study of the thermally activated delayed fluorescence (TADF) combined with aggregation-induced emission (AIE) molecular solid-state effect on the luminescence mechanism. 2023 , 811, 140257	O
121	Spodium bonding to anticrown-Hg3 boosts phosphorescence of cyclometalated-PtII complexes.	O
120	Electronic structures of zwitterionic and protonated forms of glycine betaine in water: Insights into solvent effects from ab initio simulations. 2023 , 369, 120871	O
119	Efficient enrichment of iodine by supported ionic liquid with three effective adsorption sites: Heteroatoms, fused aromatic rings and ionic bond. 2023 , 456, 140979	О
118	Highly efficient deep-blue electrofluorescence with optimized excited state composition and "hot-exciton" channel. 2023 , 210, 111002	O

117	Novel phenoxo-bridged di- and tri-nuclear Cu(II) salamo-like complexes driven by various counter-anions. 2023 , 546, 121336	O
116	Intra- and intermolecular charge transfer control of symmetric A1DA2DA1 ladder-like small molecules/g-C3N4 heterojunctions for efficient photocatalytic sterilization and degradation from visible to near-infrared. 2023, 612, 155854	O
115	Molecular level insight into the different interaction intensity between microplastics and aromatic hydrocarbon in pure water and seawater. 2023 , 862, 160786	0
114	Super-amphiphilic graphene promotes peroxymonosulfate-based emulsion catalysis for efficient oil purification. 2023 , 445, 130469	O
113	Integrated investigation for extractive denitrogenation of fuel oils with Eco-friendly Piperazine-Based ionic liquids. 2023 , 337, 127187	0
112	Anthracene separation from analogous polycyclic aromatic hydrocarbons using the naphthalene-based solvents. 2023 , 335, 127029	O
111	Solubility modeling, dissolution and solvation thermodynamics, and solutellolvent interactions of diflufenican in aqueous aprotic and protic cosolvents. 2023 , 179, 106981	0
110	Equilibrium solubility, non-covalent interactions and solvation thermodynamics of thiamphenicol in aqueous cosolvents of n-propanol/acetone/acetonitrile. 2023 , 178, 106972	O
109	How Does Spin Play with the Cycloaddition to Paramagnetic Endohedral Metallofullerenes? The Curious Case of TiSc2N@C80. 2022 , 61, 19183-19192	О
108	Theoretical insight into the acidity and cooperativity effect of the LLM-105[HNO3)2 system. 2022 , 28,	O
107	Ursolic Acid and Oleanolic Acid Dissolved in Methanol/Acetone + Water Blends: Thermodynamic Solubility, Intermolecular Interactions, and Solvation Behavior.	О
106	A theoretical study on the effects of intramolecular and intermolecular interactions on excited state properties of two NIR-TADF combined with AIE molecules. 2022 , 114000	O
105	The Chemistry of Phenylimidotechnetium(V) Complexes with Isocyanides: Steric and Electronic Factors. 2022 , 27, 8546	1
104	Probing into complexation and separation of chiral-at-uranium complex to chiral sulfur enantiomers R/S-ethiproles.	O
103	Pore Geometry and Surface Engineering of Covalent Organic Frameworks for Anhydrous Proton Conduction.	О
102	Comparative antibacterial analysis of the anthraquinone compounds based on the AIM theory, molecular docking, and dynamics simulation analysis. 2023 , 29,	O
101	Sensitivity and Weak Interaction of Energetic Ionic Salts: An Example Case of C4N18H2.	О
100	Pore Geometry and Surface Engineering of Covalent Organic Frameworks for Anhydrous Proton Conduction.	O

99	Exploring the Dynamical Nature of Intermolecular Hydrogen Bonds in Benzamide, Quinoline and Benzoic Acid Derivatives. 2022 , 27, 8847	1
98	Theoretical and experimental exploration for efficient separation of carbazole from anthracene oil with quaternary ammonium salts via forming deep eutectic solvents. 2022 , 368, 120831	Ο
97	Identification of potential inhibitors of omicron variant of SARS-Cov-2 RBD based virtual screening, MD simulation, and DFT. 10,	0
96	Trinitroaromatic Salts as High-Energy-Density Organic Cathode Materials for Li-Ion Batteries.	Ο
95	Prediction models of the ionization coefficient and ionization cross-section based on multi-layer molecular parameters.	0
94	Phase Equilibria and Mechanism Insights into the Separation of Isopropyl Acetate and Methanol by Deep Eutectic Solvents.	O
93	Unraveling the Nature of Hydrogen Bonds of P roton Sponges Based on Car-Parrinello and Metadynamics Approaches. 2023 , 24, 1542	0
92	High-capacity proton battery based on Etonjugated N-containing organic compound. 2023, 141870	Ο
91	Synthesis, Crystal Structure, and Characterization of Energetic Salts Based on 3,5-Diamino-4H-Pyrazol-4-One Oxime. 2023 , 28, 457	0
90	Thermodynamic Mechanism of Physical Stability of Amorphous Pharmaceutical Formulations.	O
89	Regulating the Reaction Pathway of nZVI to Improve the Decontamination Performance Through Magnetic Spatial Confinement Effect. 2023 , 130799	0
88	Thyroid hormone transporters binding affinity of methoxypoly chlorinated biphenyls: Insights from molecular simulations and fluorescence competitive binding experiment. 2023 , 123224	O
87	The theoretical study of the oxidation reaction of hydroxyl radical for the removal of volatile organic aliphatic and aromatic aldehydes from the atmosphere.	0
86	Bicyclic High-Energy and Low-Sensitivity Regioisomeric Energetic Compounds Based on Polynitrobenzene and Pyrazoles.	O
85	Density Functional Study of transition metal (Fe,Co,Ni) doped C60 fullerenes as 6-thioguanine delivery system.	0
84	Molecular insights into the functionalization of Au13 nanocluster with mercaptopurine anti-cancer drug. 2023 , 414547	O
83	Synthesis and characterization of potential polycyclic energetic materials using bicyclic triazole and azetidine structures as building blocks. 2023 , 13, 2600-2610	O
82	Insights into Lewis/Brfisted acidity of metal chlorides and solvent effect of alcohols for synthesis of Evalerolactone by combining molecular dynamics simulations and experiments. 2023 , 335, 126749	O

81	Experimental and theoretical study on photochromism of triphenylvinyl-naphthopyrans. 2023, 211, 111070	0
80	Application of facilitated transfer mechanisms of SEBS/[P(14)666][TMPP] composite membrane on CH4/N2 separation. 2023 , 11, 109243	O
79	Investigation of the synergetic regulation of O2/Ar preheating treatment and sodium salt addition on semichar combustion characteristics. 2023 , 338, 127269	0
78	Microscopic mechanism for the effect of potassium on heterogeneous NOI har(N) interaction: A theoretical account. 2023 , 242, 107657	O
77	Corrosion inhibition mechanism of imidazole ionic liquids with high temperature in 20% HCl solution. 2023 , 29,	1
76	Molecular structure, spectroscopic and DFT computational studies on 3,9-diazatetraasteranes.	O
75	Solvent Molecule Design Enables Excellent Charge Transfer Kinetics for a Magnesium Metal Anode. 2023 , 8, 780-789	0
74	Regulation of external electric field on the high-energy polynitrogen compound 1,5-diaminotetrazole-4[N-oxide. 2023 , 29,	O
73	Unraveling Weak Interaction of Kinematic Viscosity of Fatty Acid Methyl Esters in Natural Ester Insulating Oils. 2023 , 1-1	0
72	Theoretical exploration of noncovalent interactions in Sc2C2@C2n (n = 40 , 41 , and 42)?[12]CPP, PF[12]CPP. 2023 , 13, $4553-4563$	O
71	Construction of High-Performance Energetic MOFs: C4N8O42land C3N4O42lwith Their Derivatives, Compared with Their Energetic Salts. 2023 , 23, 820-831	0
70	Construction of Efficient DA-Type Photocatalysts by BN Bond Substitution for Water Splitting.	O
69	Chemical insights from the Source Function reconstruction of scalar fields relevant to chemistry. 2023 , 269-333	0
68	Dissecting amide-I vibrations in histidine dipeptide. 2023 , 292, 122424	O
67	Computational Investigation of Stability and Molecular Properties of C18BN Corannulene Molecules. 2022 , 67, S158-S168	0
66	Why does the cyclic pentazolate anion fail to undergo N-oxidization in oxone solution?. 2023 , 47, 5616-5620	O
65	Terahertz spectroscopic characterization and DFT calculations of vanillin cocrystals with nicotinamide and isonicotinamide. 2023 , 25, 2038-2051	0
64	Lead Sequestration in Perovskite Photovoltaic Device Encapsulated with Water-Proof and Adhesive Poly(ionic liquid). 2023 , 15, 13637-13643	O

63	Covalent Triazine Framework C6N6 as an Electrochemical Sensor for Hydrogen-Containing Industrial Pollutants. A DFT Study. 2023 , 13, 1121	0
62	Mixing behavior of 1-Ethyl-3-methylimidazolium Bis(trifluoromethylsulfonyl)imide and 1-Ethyl-3-methylimidazolium tetrafluoroborate binary ionic liquids mixtures. 2023 , 569, 111858	O
61	Pectin grafted with resorcinol and 4-hexylresorcinol: Preparation, characterization and application in meat preservation. 2023 , 237, 124212	O
60	Study on mechanism of cellulose hydrolysis during alkali thermal pretreatment of lignocellulose by density functional theory. 2023 , 172, 106754	O
59	A novel binary solid-liquid biphasic functionalized ionic liquids for efficient CO2 capture: Reversible polarity and low energy penalty. 2023 , 313, 123486	O
58	The rapid and sensitive detection of trace copper ions by L-cysteine capped ZnS nanoparticle fluorescent probe and the insight into micro-mechanism: Experiments and DFT study. 2023 , 294, 122570	O
57	Impact of silica nanoparticles architectures on the photosensitization of O2 by immobilized Rose Bengal. 2023 , 440, 114648	O
56	A copolyether with pendant cyclic carbonate segment for PEO-based solid polymer electrolyte. 2023 , 570, 233049	O
55	Exploring the structural, photophysical and optoelectronic properties of a diaryl heptanoid curcumin derivative and identification as a SARS-CoV-2 inhibitor. 2023 , 1281, 135110	O
54	Experimental and quantum chemical investigations on the generation mechanism of Al-V intermediate alloy by aluminothermic reduction of NaVO3. 2023 , 945, 169252	O
53	Computational characteristics of the structure-activity relationship of inhibitors targeting Pks13-TE domain. 2023 , 104, 107864	O
52	The prediction and assessment of properties for high energy density fuel Adamantane derivatives: The combined DFT and molecular dynamics simulation. 2023 , 343, 127975	O
51	Mechanism-driven moderate alkalinity release for efficient recovery of high-purity cobalt and nickel from spent lithium-ion batteries. 2023 , 315, 123645	O
50	Theoretical study on the mechanism of aggregation-induced emission in red thermally activated delayed fluorescence molecules: trans/cis-arrangement effect. 2023 , 119, 106811	O
49	The immobilization of Sr(ll) and Co(ll) via magnetic easy-separation organophosphonate-hydroxyapatite hybrid nanoparticles. 2023 , 315, 123750	O
48	3,4,5-Trimethoxycinnamic acid in aqueous co-solvent solutions of isopropanol/acetone/methanol/ethanol: Solubility, preferential solvation and intermolecular interactions. 2023 , 183, 107055	O
47	Main/side chain asymmetric molecular design enhances charge transfer of two-dimensional conjugated polymer/g-C3N4 heterojunctions for high-efficiency photocatalytic sterilization and degradation. 2023 , 641, 619-630	0
46	Direct synthesis of high silica SSZ-16 zeolite with extraordinarily superior performance in NH3-SCR reaction. 2023 , 332, 122746	O

45	Bisacodyl in aqueous co-solvent solutions of isopropanol/methanol/ethanol: Solubility modeling, preferential solvation and density functional theory study. 2023 , 183, 107054	0
44	Mechanism of acid-catalyzed pyrolysis of levoglucosan: Formation of anhydro-disaccharides. 2023 , 345, 128242	O
43	Experimental and computational investigation of complexing agents on copper dissolution for chemical mechanical polishing process. 2023 , 664, 131142	0
42	Bifunctional solvent-driven hydrodechlorination of 1,2-dichlorohexafluorocyclopentene and mechanism study. 2023 , 266, 110091	O
41	Computational investigations on the 4Eyanopyridine adsorbed on ZnOgraphene oxide nanocomposite toward the efficient performance of surfaceEnhanced Raman scattering. 2023, 133, 109693	О
40	Mechanism analysis and liquid-liquid equilibrium of methyl tert-butyl ether separation from petroleum wastewater azeotrope by green mixed solvent. 2023 , 11, 109389	1
39	Anion recognition using enhanced halogen bonding through intramolecular hydrogen bonds la computational insight. 2023 , 47, 4439-4447	O
38	Is chitin a promising hydrogen storage material? A thorough quantum mechanical study. 2023,	Ο
37	Methylthiazole Schiff base functionalized SBA-15 for high-performance Pb(II) capture and separation. 2023 , 351, 112476	Ο
36	Tuning Ion Transport at the Anode-Electrolyte Interface via a Sulfonate-Rich Ion-Exchange Layer for Durable Zinc-Iodine Batteries. 2023 , 13,	O
35	Preparation of nano disperse dyes using sulfomethylated lignin: Effects of sulfonic group contents. 2023 , 234, 123605	0
34	Electrochemical Removal of NiEDTA Mediated by Chlorine and Hydroxyl Radicals on BDD Anodes. 2023 , 3, 827-837	O
33	Novel class of crown ether functionalized ionic liquids with multiple binding sites for efficient separation of lithium isotopes. 2023 , 376, 121412	0
32	Enhancing cation storage performance of layered double hydroxides by increasing the interlayer distance. 2023 , 158, 094703	O
31	Energetics and Ionic E lectronic and Geometric Variabilities of Hydroxylammonium-Based Salts. 2023 , 23, 1821-1831	O
30	Facile Synthesis of Energetic Multi-Heterocyclic Compound via a Promising Intramolecular Integration Strategy. 2023 , 23, 2721-2729	O
29	Trapping of Small Molecules within Single or Double Cyclo[18]carbon Rings. 2023, 28, 2157	0
28	Comparative study of the hydrogen bonding interactions between ester-functionalized/non-functionalized imidazolium-based ionic liquids and DMSO. 2023 , 25, 8789-8798	O

27	Electrical Breakdown Mechanism of ENB-EPDM Cable Insulation Based on Density Functional Theory. 2023 , 15, 1217	О
26	Experimental and Theoretical Investigation of Hydrogen-Bonding Interactions in Cocrystals of Sulfaguanidine. 2023 , 23, 2306-2320	О
25	Activation of metal-involved halogen bonds and classical halogen bonds in gold(i) catalysis. 2023 , 52, 4517-4525	О
24	Microscopic Mechanism of Electrical Aging of PVDF Cable Insulation Material. 2023, 15, 1286	O
23	Bis(perfluoroaryl)chalcolanes ArF2Ch (Ch = S, Se, Te) as ÆHole Donors for Supramolecular Applications Based on Noncovalent Bonding. 2023 , 23, 2593-2601	О
22	Use the Functional Electrolyte Containing 2-Propynemethanesulfonate or 2-Propynebenzenesulfonate Additives to Improve the Long-Cycle Performance of LiNi0.8Co0.1Mn0.1O2/Graphite Batteries. 2023 , 170, 030526	O
21	O,S-Acetals in a New Modification of oxo-Friedel@raftsBradsher CyclizationBynthesis of Fluorescent (Hetero)acenes and Mechanistic Considerations. 2023 , 28, 2474	O
20	Smoothing Energy Transfer Enabling Efficient Large-Area Quasi-2D Perovskite Light-Emitting Diodes. 2200847	O
19	A Comprehensive Investigation into the Crystallology, Molecule, and Quantum Chemistry Properties of Two New Hydrous Long-Chain Dibasic Ammonium Salts CnH2n+8N2O6 (n = 35 and 37). 2023 , 24, 5467	О
18	Combination of Energetic Tetrazole and Triazole: Promising Materials with Exceptional Stability and Low Mechanical Sensitivity as Propellants and Gas Generators. 2023 , 15, 15311-15320	O
17	The selective and sustainable separation of Cd(II) using C6MImT/[C6MIm]PF6 extractant. 2023, 255, 114792	O
16	Vitamin B 1 -Catalyzed Multicomponent Reaction for Efficient Synthesis of an Isoxazolone Compound by Using Ultrasound in a Water and Its Selective Identification of Metal Ions. 2023 , 8,	О
15	meso-Carbazole decorated BODIPYs han electron donor ceptor system with excellent fluorosolvato/vapochromic behavior, aggregation-induced emission, and antileishmanial activity.	O
14	Study of the reaction mechanism based on the formation of the first carbocyclic ring from propargyl and diacetylene. 2023 , 51, 492-501	O
13	Solvent Effect on the Nonlinear Optical Property in Cr(CO)3L Complexes (L = 🔁-Benzene and 🖺-Graphene): A Theoretical Study. 2023 , 17, 27-35	O
12	Monitoring amyloid aggregation via a twisted intramolecular charge transfer (TICT)-based fluorescent sensor array.	O
11	Searching for the analogues of 1,1-dinitro-2,2-diamino ethylene (FOX-7) by high-throughput computation and machine learning. 2023 ,	0
10	Photoactivated organic phosphorescence by stereo-hindrance engineering for mimicking synaptic plasticity. 2023 , 12,	O

CITATION REPORT

9	MOF-derived Co/Fe@NPC-500 with large amounts of low-valent metals as an electro-Fenton cathode for efficient degradation of ceftazidime. 2023 , 333, 122755	O
8	Influence Mechanism of Polymeric Excipients on Drug Crystallization: Experimental Investigation and Chemical Potential Gradient Model Analysis and Prediction.	O
7	An Aromaticity Study of Localized and Non-Localized Orbitals in \$\$B_{3}^{{n mp ,0}}\$\$, \$\$B_{4}^{{n mp ,0}}\$\$, \$\$B_{6}^{{n mp ,0}}\$\$, and \$\$B_{7}^{{n mp ,0}}\$\$ (n = 0, 1, 2) Rings. 2023 , 97, 151-167	О
6	Prediction, Application, and Mechanism Exploration of Liquid Liquid Equilibrium Data in the Extraction of Aromatics Using Sulfolane. 2023 , 11, 1228	O
5	Stabilization of 2-Pyridyltellurium(II) Derivatives by Oxidorhenium(V) Complexes. 2023, 5, 934-947	O
4	Synthesis, crystal structure, biological evaluation, docking study and DFT calculation of novel strobilurins containing oxime ether phenyl ring or dihydrobenzofuran moiety. 2023 , 135636	O
3	Static and Dynamical Quantum Studies of CX3-AlX2 and CSiX3-BX2 (X = F, Cl, Br) Complexes with Hydrocyanic Acid: Unusual Behavior of Strong Hole at Triel Center. 2023 , 24, 7881	Ο
2	DFT investigation of stability, electronic and optical properties of coordination of C20 corannulene to Fe(CO)4. 2023 , 153, 110793	O
1	Unraveling complexation and separation of novel asymmetric uranyl-5-methoxy-2-(4-methoxy-6[(quinazolin-2-yl)-[2,2Ebipyridin]-6-yl) quinazoline to chiral fungicides R/S-metalaxyls and R/S-benalaxyls. 1-18	O